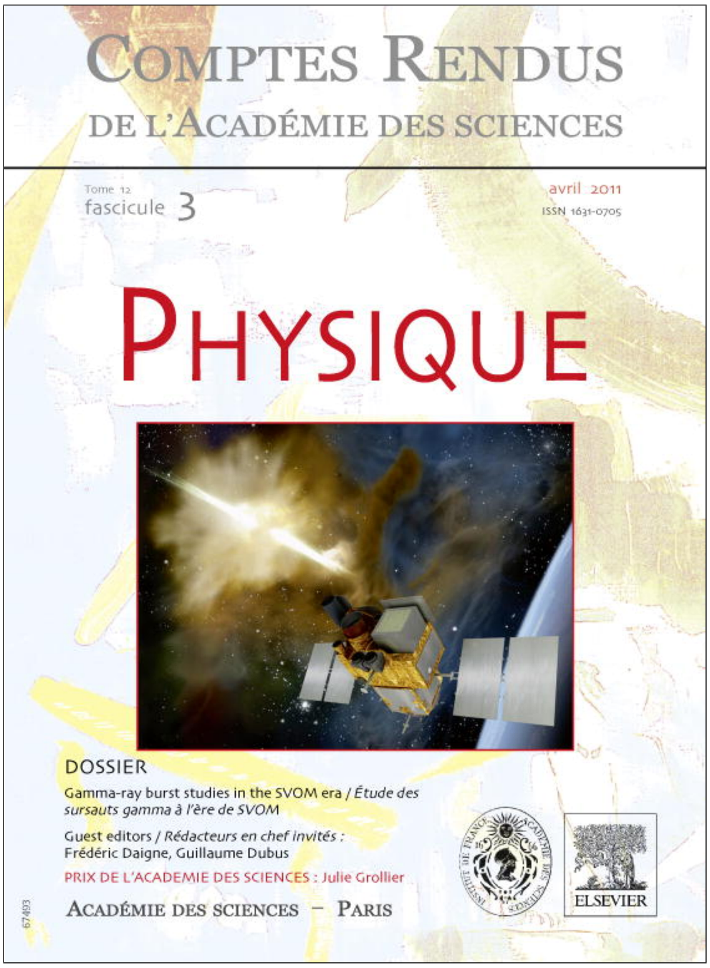
COMPTES RENDUS
DE L'ACADÉMIE DES SCIENCES
Tome 12
fascicule 3
avril 2011
ISSN 1631-0705
PHYSIQUE
DOSSIER
Gamma-ray burst studies in the SVOM era / Étude des sursauts gamma à l'ère de SVOM
Guest editors / Rédacteurs en chef invités :
Frédéric Daigne, Guillaume Dubus
PRIX DE L'ACADEMIE DES SCIENCES : Julie Grollier
ACADÉMIE DES SCIENCES – PARIS
ELSEVIER

C. R. Physique 12 (2011) 206–225

Contents lists available at ScienceDirect

Comptes Rendus Physique

www.sciencedirect.com

Gamma-ray burst studies in the SVOM era / Étude des sursauts gamma à l'ère de SVOM

Open questions in GRB physics

Questions ouvertes de la physique des sursauts gamma

Bing Zhang

Department of Physics and Astronomy, University of Nevada, Las Vegas, NV 89154, USA

ARTICLE INFO

Article history:
Available online 13 April 2011

Keywords:
Gamma-rays, bursts
Stars
Black holes
Neutron stars
Shocks
Magnetic fields
Radiation mechanism

Mots-clés :
Sursauts gamma
Étoiles
Trous noirs
Étoiles à neutrons
Chocs
Champs magnétiques
Processus de rayonnement

ABSTRACT

Open questions in GRB physics are summarized as of 2011, including classification, progenitor, central engine, ejecta composition, energy dissipation and particle acceleration mechanism, radiation mechanism, long term engine activity, external shock afterglow physics, origin of high energy emission, and cosmological setting. Prospects of addressing some of these problems with the upcoming Chinese–French GRB mission, SVOM, are outlined.

RÉSUMÉ

Cette contribution résume les questions ouvertes de la physique des sursauts gamma, début 2011. La classification, les progéniteurs, le moteur central, la composition de l'éjecta, la dissipation d'énergie et les mécanismes d'accélération de particules, les processus de rayonnement, l'activité prolongée du moteur central, la physique du choc externe lors des rémanences, l'origine de l'émission haute énergie et le contexte cosmologique sont successivement évoqués. L'apport attendu de la mission franco-chinoise SVOM à la résolution de certaines de ces questions est ensuite expliqué.

1. Introduction

The field of gamma-ray bursts (GRBs) has rapidly advanced in recent years, especially following the launches of NASA missions *Swift* (in 2004) and *Fermi* (in 2008) [1–4]. Due to their elusive nature, observing GRBs in all wavelengths at all epochs (including during and after the GRB) is still challenging with the current GRB detectors and follow up telescopes. As a result, every time a new temporal or spectral window is unveiled, a rich trove of new phenomenology is uncovered. While solving some old problems, new observations usually raise more questions and challenges. This provides sustainable impetus to this still relatively young field. In any case, current observations gradually put together a sketch of the global picture of GRBs, although many details remain vague or uncertain.

This review summarizes the open questions in GRB physics as of 2011. Ten topics are discussed, including classification, progenitor, central engine, ejecta composition, energy dissipation and particle acceleration mechanism, radiation mechanism, long term engine activity, external shock afterglow physics, origin of high energy emission, and cosmological setting. In connection with the upcoming Chinese–French SVOM (Space-based multi-band astronomical Variable Object Monitor) mission,

E-mail address: zhang@physics.unlv.edu.

1631-0705/$ – see front matter
doi:10.1016/j.crhy.2011.03.004

I also discuss some prospects of addressing some of these problems in 2015 and beyond. More detailed discussions on the SVOM mission [5] and multi-wavelength observational prospects in 2015 and beyond [6] can be found in this issue.

2. Open questions

2.1. Classification

In astronomy, classification is traditionally solely based on distinct clusters in data based on well-defined criteria. Well known examples include stellar spectral classification and supernova classification, both having spectral line features as essential criteria. Since these criteria usually invoke "yes" or "no" judgments, the classification schemes of these objects are relatively unambiguous. As transient events without any credible spectral feature, the GRB classification was traditionally based on their durations in the temporal domain and hardness ratio (HR) in the spectral domain. An analysis of GRBs detected by BATSE (sensitive in 30 keV–2 MeV) suggested that there are two classes of GRBs in the T_{90}–HR space, i.e. the long/soft class that comprises roughly 3/4 of the population, and the short/hard class that comprises the other 1/4 [7]. A rough separation line in duration, i.e. $T_{90} \sim 2$ s in the observer frame, was suggested.

The main issue of applying the T_{90} criterion to define the class of a GRB is that T_{90} is detector dependent. GRB pulses are typically broader at lower energies. Also a more sensitive detector tends to detect weaker signals which would be otherwise buried in noises. It was therefore not surprising that observations carried out with softer detectors such as HETE-2 and *Swift* brought confusions to classification. For example, among a total 476 GRBs detected by *Swift* BAT (sensitive in 15–150 keV) from Dec. 19, 2004 to Dec. 21, 2009, only 8% have $T_{90} < 2$ s [8], much less than the $\sim 1/4$ fraction of the BATSE sample. An additional 2% of *Swift* GRBs have a short/hard spike typically shorter than or around 2 s, but with an extended emission lasting 10's to ~ 100 s. These bursts, dubbed "short GRBs with E.E." [9], have $T_{90} \gg 2$ s as observed by *Swift*, but could be short GRBs if they were detected by BATSE. So the unfortunate consequence of the T_{90} classification is that the membership to a certain category of the *same* GRB could change when the detector is changed. One possibility is to define a burst's category based on its BATSE-band duration. Then two issues arise: First, what is special for the BATSE band? If other detectors such as *Swift* were launched earlier, what would be the criteria to define long vs. short GRBs? Second, it is difficult to precisely infer T_{90} in the BATSE band using the data of other detectors (e.g. *Swift*/BAT). It requires accurate time-dependent spectral information of the entire burst, which is only available for few very bright GRBs. Even for these bursts, extrapolating the BAT band spectrum to the BATSE regime is risky and usually not correct, since the GRB spectrum is known to be curved. This has been evidenced in some *Swift* GRBs that were co-detected by other detectors with harder bandpass such as Konus/Wind. Fortunately, the confusion in T_{90} classification only arises in the "grey" area between the two classes. For most GRBs, one can still tell whether they are "long" or "short".

A further complication is that several groups argue that the best fit to the T_{90} distribution histogram is three Gaussian functions in logarithmic space, e.g. [10]. This adds one more "intermediate-duration" class besides the traditional "short" and "long". For the same GRB, the membership to this intermediate class is even more ambiguous and subject to the detector bandwidth and sensitivity.

The differentiation between long and short GRBs is established with a firmer footing thanks to the afterglow and host galaxy observations. Observations led by BeppoSAX, HETE-2, and *Swift* suggest that at least some long GRBs are associated with supernova Type Ic [11–15]. Most long GRB host galaxies are found to be dwarf star-forming galaxies [16]. These facts establish the connection between long GRBs and deaths of massive stars [17,18]. The breakthrough led by *Swift* unveiled that some nearby short GRBs (or short GRBs with E.E.) have host galaxies that are elliptical or early type, with little star formation [19–22]. This points towards another type of progenitor. The top candidate model for this category is mergers of two compact objects, e.g. two neutron stars (NS–NS) or a neutron star and a black hole (NS–BH) [23–25]. This led to the common ansatz that "long GRB = massive star GRB, and short GRB = compact star GRB".

Such a cozy picture was soon messed up by some observations. GRB 060614 and GRB 060505 are two long duration nearby GRBs that did not have bright SN associations and that share similar properties to short GRBs [26–30]. Two high-z GRBs 090423 and 080916 have rest-frame durations shorter than 1 s, but are likely related to massive stars [31–34]. An observer-frame short GRB 090426 was found in many aspects similar to long GRBs [35–37]. This suggests that certain observation properties (e.g. long vs. short duration) do not always refer to certain types of progenitor.

While some appeal to modify the meaning of "long" and "short" to reflect "massive star origin" and "compact star origin",[1] respectively, others started to "classify" GRBs physically [30,38,31], and appeal to multiple observational criteria to determine the "physical category" of a GRB [39,31]. The classification here is beyond the traditional definition of astronomical classifications (which are based on data). Rather, they are based on some well-motivated GRB progenitor models which are believed to be associated with GRBs (see more discussion below in Section 2.2). For cosmological GRBs that mark catastrophic explosions, two general physical classes of GRBs (or two types of models that are associated with GRBs) are "massive star GRBs" (or "Type II GRBs") and "compact star GRBs" (or "Type I GRBs") [30,38,31,40,41]. Since duration alone is no longer necessarily a good indicator for the physical category of a GRB, one must appeal to multiple observational criteria to judge the correct physical category of the GRB progenitor model that is associated with a certain GRB [31,39].

[1] The "long" and "short" notations become more and more confusing, since growing data demand to introduce more complicated notations such as "long short GRBs" or "short long GRBs".

One may also seek for other observational parameters to conduct GRB classification. For example, for GRBs with redshift measurements, a parameter $\varepsilon \equiv E_{\gamma,\mathrm{iso},52}/E_{p,z,2}^{5/3}$ can be used to classify GRBs into two categories [42]. The high-ε and low-ε categories are found to be more closely related to Type II (massive star) GRBs and Type I (compact star) GRBs, respectively.

2.2. Progenitor

The progenitors of GRBs are not identified, and it will be very difficult to identify them. There are two ways to approach this goal. One is to use observational data to narrow down the allowed progenitor types. The other is to use theoretical insights to construct toy models (e.g. collapse of a massive star, merger of two NSs) and use analytical and numerical methods to investigate whether GRBs can be made.

For massive star GRBs (typically long), the following two observational facts have offered important clues for the progenitor type: (1) A handful of GRBs are found to be associated with supernovae Type Ic (no hydrogen lines and no or weak helium lines) [11–15,43]; (2) The hosts are dwarf galaxies with intense star formation, and the GRB locations track the brightest star formation regions in the hosts [16,44]. Theoretically, in order to produce a relativistic jet from a collapsing star to power the observed GRB, one requires that the stellar core must carry a high angular momentum [45]. The spin axis then provides a natural preferred direction for jet launch and propagation.

One then comes up with three requirements for a massive star GRB progenitor: (1) These stars must track the brightest regions in the star formation regions; (2) The hydrogen envelope is largely depleted so that the progenitor is likely a Wolf–Rayet star; (3) The core carries a high angular momentum. Within these general constraints, several candidate progenitor systems are possible [46]: collapse of a massive single star with a high angular momentum; collapse of a massive star in a close binary system; and merger of two He stars. For the single star scenario, achieving both a depleted hydrogen envelope (which requires a strong wind, and hence, high metallicity) and a rapidly rotating core (requires low metallicity) seem contradictory. It is argued that rapid mixing of H with He would result in burning H to He without the need of ejecting the H envelope (and hence without losing angular momentum) [47]. Alternatively, a binary progenitor can retain a high angular momentum core with the H envelope ejected [45].

An alternative idea to interpret massive star GRBs is to invoke two-step explosions. Such a “supranova” model [48] envisages a core collapse supernova explosion weeks to months before the GRB. This first explosion produces a rapidly rotating massive neutron star, which subsequently collapses to form a black hole and generates a GRB later when the centrifugal support is not enough to hold the neutron star. The observed GRB/SN associations suggest that the delay between the SN and GRB, if any, cannot be more than 1–2 days [12–15,43]. This model is therefore not favored for massive star GRBs.

One should keep in mind the following caveats regarding the massive star progenitors in general: (1) Among 5–6 robust cases of GRB/SN associations, only GRB 030329 is a typical GRB. The rest are nearby, low luminosity GRBs, which may form a distinct population with a different progenitor or different central engine [49–51]. Strictly speaking, we are relying on one case to speculate the progenitor of most GRBs. It is possible that all high luminosity GRBs are associated with SNe. Observationally the SN signature is however difficult to catch, since these GRBs are usually not at low redshifts, and since they typically have bright optical afterglows to outshine the SN signals. (2) A good fraction of long GRBs, namely “optically dark GRBs”, do not have a detectable optical afterglow. Their host galaxies are usually not identified. The predominant dwarf star-forming host galaxies in the published sample [16] may be due to a selection effect. In fact, a *Chandra* observation of the dark GRB 090417B shows that its host galaxy is a Milky Way like galaxy with heavy dust extinction [52]. (3) The theoretical preference of low metallicity (to retain angular momentum) is not fully established from the data [44], although various arguments have been made in favor of such a condition [53–55].

The observational evidence for a compact star merger progenitor is indirect (in contrast to the massive star progenitor), which is based on the following observational facts: (1) GRB 050509B and GRB 050724 are found to be associated with an elliptical host galaxy (the former) or an early type host galaxy with low star formation rate (the latter) [19,56,21,22]; (2) Statistically, most identified short GRB hosts are late type galaxies, but GRBs track less bright regions of the galaxies, and have larger offsets from the centers [57]; (3) Deep searches placed stringent upper limits on supernova light associated with several nearby short GRBs [56,20,22,58,41]. Theoretically, compact star mergers would have much less and much denser fuel than massive star core collapses, which would power short duration GRBs [59–61].

The two popular models involving compact star mergers include NS–NS mergers [23–25] and NS–BH mergers [62]. The double NS systems are known to exist in our galaxy, and their orbits are known to shrink due to gravitational radiation [63,64]. They are doomed to merge someday, so the NS–NS merger model has been the earliest cosmological model for GRBs. The NS–BH binary systems are not observed. This does not necessarily mean that they are much rarer than NS–NS systems (although they should be rarer). This is because at least one pulsar is expected to be “recycled” in the NS–NS system, so that its radio beam is much wider than normal PSRs and detections are eased. The pulsar in the BH–NS system, however, is not expected to go through this recycling phase, so that the pulsar detectability is significantly lower. In any case, both merger models are argued to be able to interpret many short GRB properties (see [65,66] for reviews).

Despite the indirect supports to the merger scenarios mentioned above, the following observational facts raise caution to take the merger progenitors as truth. First, a group of short GRBs are found to have redshifts > 1 [67], some having luminosity typical for long GRBs [68]. Some apparent long GRBs, including the two highest-z GRBs [32–34], have rest-frame duration shorter than 1 s. The high energetics of these GRBs demands extremely narrow beaming of the NS–NS progenitor, which is difficult to achieve theoretically. Numerical modeling consistently reveals wide jets in merger systems due to the lack of a dense medium (e.g. the stellar envelope as expected in massive star core collapse scenarios) to help to collimate the jet [60,61]. Only BH–NS systems powered by BH spin may power these energetic events, but these mergers (with a massive BH and rapid BH spin) are very rare. Second, in order to account for many high-L short GRBs and not-too-many low-L nearby short GRBs, the luminosity function of short GRBs should be shallow [69]. Since most merger models predict a redshift-distribution that peaks at low-z, the shallow luminosity function is translated to a shallow peak flux distribution ($\log N$–$\log P$), which violates the BATSE short GRB sample constraint significantly [69]. The consistency between the merger models and the *Swift* z-known sample [70] or the BATSE sample [71] was claimed shortly after the discovery of short GRB afterglows. However, the *Swift* sample was too small and the two samples (*Swift* vs. BATSE) were not jointly considered in those analyses. A recent joint analysis shows a sharp inconsistency between various merger models and the observational constraints (z–L distributions and $\log N$–$\log P$ distributions) [69]. This may suggest that either the merger models are not the correct model for short GRBs, or not all short GRBs are from compact star mergers. A recent modified compact star coalescence scenario is to invoke dynamical "collisions" of NS–NS or NS–BH systems in globular clusters [72, 73]. If this population of coalescences dominates over mergers in the field galaxy due to gravitational wave radiation, the above conflict may be alleviated. In any case, since NS–NS and NS–BH merger models predict specific gravitational wave signals [74], a definite test to the merger models of short GRBs may be achieved in the future when gravitational wave detections become possible.

Besides mergers, several other types of progenitor have been proposed for short GRBs. One scenario is accretion-induced-collapses (AICs) of NSs (e.g. [75]), which is similar to the "supranova" model for long GRBs [48], but with a much longer delay between the SN and GRB. Cosmological short GRBs may be produced this way. Soft Gamma-ray Repeaters (SGRs) produce giant flares with a short, hard spike, which would be recognized as short/hard GRBs in nearby galaxies [76–78]. It is likely that the short/hard GRB population is contaminated by these events, but the fraction of contamination is believed to be small [79].

2.3. Central engine

Different types of progenitor may result in a common central engine that powers the observed GRBs. Observations suggest that a GRB central engine should satisfy the following requirements: (1) It can drive an outflow with extremely high luminosity and energy. If the emission is isotropically distributed in all directions, the required jet luminosity ranges from $L_{\rm iso} \sim 10^{47}$–10^{54} erg s^{-1}, and the total gamma-ray energy ranges from $E_{\rm iso} \sim 10^{49}$–10^{55} erg [80,81]; (2) The ejecta need to be "clean" with small baryon contamination, so that they can achieve a relativistic speed, with Lorentz factor Γ typically greater than 100 [82–84], some even close to 1000 [85–87]; (3) The outflow needs to be collimated, with a beaming factor $f = \Delta\Omega/4\pi \sim 1/500$ for bright GRBs [88–91], so that the real luminosity and energy of a GRB is reduced by this factor; (4) The engine needs in general to be intermittent, with a range of variability time scales [80,92]. In some GRBs, the engine can generate smooth (but varying) lightcurves [93,14]; (5) The engine can last long, with renewed, progressively less powerful late activities to power X-ray flares and other activities (see Section 2.7 for full discussion).

Several types of GRB central engine have been discussed in the literature. The leading candidate is a black hole (possibly rapidly spinning) + torus system. An alternative candidate is a rapidly spinning, highly magnetized NS (magnetar). A more exotic possibility is a compact star solely composed of quark matter, i.e. a quark star. There are three energy reservoirs involved in these engines: the accretion power, the spindown power of the central object, and the phase transition power.

The black hole–torus engine is widely discussed in both the collapsar scenario [17,94–96], and the compact star merger scenario [25]. The first energy source is the accretion power from the torus. Neutrino annihilation from the torus can drive a hot jet along the spin axis to power the GRB. The accretion powered jet luminosity is $L_{\rm acc} = \zeta \dot{M} c^2 \sim 1.8 \times 10^{51}$ erg s^{-1} $\zeta_{-3}(\dot{M}/1 M_\odot\ {\rm s}^{-1})$. In order to achieve the observed GRB luminosity, the accretion rate should be close to $(0.1\text{–}1) M_\odot/{\rm s}$ for a reasonable efficiency factor ζ to convert accretion power into jet power. The second energy source is the spin energy of the black hole. This energy can be tapped by magnetic fields threading the ergosphere of a Kerr black hole through the Blandford–Znajek (BZ) mechanism [98–102]. The jet luminosity $L_{\rm BZ} \simeq 0.1 B^2 (\Omega_{\rm BH}^2/c)(GM_{\rm BH}/c^2)^2 \simeq 3 \times 10^{50}$ erg s^{-1} $B_{15}^2 (M/3M_\odot)^2 a^2 f(a)$, where a is the dimensionless spin parameter of the black hole, and $f(a)$ is a increasing function of a. In order to power a GRB, the black hole should be rapidly spinning ($a \lesssim 1$), the accretion rate should be high so that magnetic fields near the horizon are strong enough (the radial magnetic field strength near the black hole is $B \gtrsim 10^{15}$ G). For a same a, a more massive BH (and hence, more spin energy to tap) would give a more luminous burst. Such a BZ-powered jet would carry a strong magnetic field, and is likely Poynting-flux-dominated. It is possible that both mechanisms (neutrino annihilation and BZ process) are operating in BH–torus systems. A variable outflow can be due to the interplay between the magnetic fields and the accreting materials [103,104]. For a jet emerging from a star, jet propagation instabilities in the envelope can give rise to further variabilities in the outflow [96,97].

The main power of a millisecond magnetar engine is its spindown power [105], which is $L_{\rm sd} = B^2 \Omega^4 R^6/6c^3 \sim 3.7 \times 10^{50}$ erg s^{-1} $B_{15}^2 \Omega_4^4 R_6^6$ for the dipole spindown model. In order to power a GRB, the magnetar must have a surface magnetic field $B \gtrsim 10^{15}$ G, and an angular frequency $\Omega \gtrsim 10^4$ Hz (which corresponds to a spin period $P \lesssim 0.6$ ms). Notice that $\Omega \sim 10^4$ is already close to the upper limit of the angular frequency of a neutron star. The maximum total energy of a magnetar engine is defined by its spin energy $E_{\rm spin} \sim (1/2) I \Omega^2 \sim 5 \times 10^{52}$ erg. Increasing B would reduce the spindown time scale $\tau_{\rm sd} = 3c^3 I/(B^2 R^6 \Omega^2) \simeq 800\ {\rm s}\ I_{45} B_{15}^{-2} R_6^{-6} \Omega_4^{-2}$. In principle, the engine cannot power an intrinsically luminous and long GRB. One may invoke a small beaming factor f to accommodate a large isotropic luminosity. However, for millisecond rotators the open field lines have a large solid angle, so that f cannot be too small unless another medium (e.g. envelope or supernova ejecta) serve to collimate the jet. It is possible that the accretion power also operates in a magnetar. The neutrino annihilation rate is enhanced with respect to the BH–torus system [106]. However, given the high accretion rate (e.g. $1M_\odot/\mathrm{s}$), the NS would quickly (e.g. in 2 s) turn into a BH. Another issue is that a neutrino-driven wind from a proto-neutron star tends to be "dirty" [107,108], which cannot produce a clean fireball to power a GRB. A GRB may be generated after the proto-neutron star cools and a Poynting flux dominated outflow is launched, typically several seconds later [109–111]. Scenarios to have a magnetic bubble penetrating through the stellar envelope without significant contamination have been discussed [112,113].

Strange quark matter could be more stable than neutron matter [114], so that strange quark stars could form in high pressure environments for a wide range of allowed parameters for QCD [115]. A quark star engine has been invoked to power a GRB in various contents [116–120]. There are two advantages of introducing a quark star engine. First, extra energy sources due to phase transitions (from neutron matter to 2-flavor quark matter, from 2-flavor to 3-flavor strange quark matter, and quark matter condensation [116,118,120]) are introduced. Second, since the star is bound by strong interaction rather than gravity, neutrinos and photons can be released without launching materials to contaminate the fireball [116,118,119]. The time scale for phase transitions may be fast. In order to launch a highly variable jet, intermittent accretion is needed, and the engine power includes both the accretion power and the phase transition power [118].

Since all three types of engine are argued to satisfy most observational constraints, identifying the right one among them using observational data is not straightforward. Among the three possible engines, the BH–torus system is most naturally expected. For massive star GRBs, studies of Type Ic SNe associated with some GRBs suggest a large enough mass for the progenitor star to form a BH rather than a NS [121,122]. A BH–torus engine is relevant for BH–NS mergers. For NS–NS mergers, the total mass of the two NSs ($\sim 2.8M_\odot$) is believed to exceed the maximum NS mass for most NS equation of state, so that a BH–torus engine is also likely. Nonetheless, evidence of a NS (QS) engine in some GRBs is collected. First, spectral modeling of SN 2006aj associated with GRB 060218 suggests that this SN has much smaller ejecta mass and kinetic energy than other Type Ic SNe associated with GRBs, pointing towards a massive star progenitor that is not massive enough to produce a BH [50]. Second, the spin down luminosity of a NS (QS) should have a constant luminosity plateau followed by a $L \propto t^{-2}$ decay. This signature may show up in the early afterglow phase. The continuous injection of pulsar spindown energy onto the blastwave would result in a shallow decay phase in the early afterglow phase [123,124], which may account for the plateau feature in the early afterglows of some *Swift* GRBs [125–127]. If the pulsar wind has strong dissipation before landing on the blastwave and if the engine ceases suddenly (probably due to collapse into a black hole), an "internal plateau" would appear in the X-ray afterglow, characterized by a plateau phase followed by a very steep decay as observed in some *Swift* GRBs [128–130] (see Section 2.7 for more discussion). We therefore suggest that although BH–torus systems may be common in most bright, energetic GRBs, pulsar systems may exist in at least some GRBs. Unfortunately, besides theoretical arguments, there is essentially no "smoking-gun" observational criterion to differentiate a QS engine from a NS engine.

A dedicated review on numerical simulations of GRB central engines can be found in this issue [131].

2.4. Ejecta composition

The composition of a GRB outflow includes three components: matter, magnetic fields, and photons. Photons are advected with matter and magnetic fields initially, and are decoupled from the ejecta at the photosphere radius, where Compton scattering optical depth drops below unity. Above the photosphere, the jet carries a matter flux and a magnetic flux, which is essentially a Poynting flux in the lab frame because of the existence of an induced electric field. More photons are generated from the regions where kinetic energy or magnetic energy is dissipated (i.e. shocks or magnetic reconnection regions), which escape the ejecta without further coupling. The distribution of energy between matter and magnetic fields is denoted by the magnetization factor $\sigma \equiv B^2/4\pi \Gamma \rho c^2$ (where the magnetic field B and the matter density ρ are measured in the lab frame), the ratio between Poynting flux and matter flux. Within the matter content, one has the baryonic and leptonic components. The relative distribution can be denoted by a parameter $Y = n_\pm/n_p$, the number ratio between leptons and protons. Usually the baryonic component dominates in mass unless $Y \geqslant m_p/m_e$, the proton-to-electron mass ratio. Due to the extreme temperature (typically $kT \sim$ MeV) and density (typically nuclear density) at the central engine, heavy ions are less likely to survive in the jet, so the dominant charged baryons in the jet are protons. For both compact star merger and massive star core collapse central engines, it is likely that a noticeable fraction of free neutrons exist in the fireball, and initially are coupled with protons through strong interaction [132,133]. These neutrons decouple from the ion ejecta, decay with a comoving life time ~ 900 s, and would leave interesting observational features [132,134,135]. The abundance of free neutrons is usually denoted by the neutron-to-proton number ratio, $\xi \equiv n_n/n_p$.

The traditional GRB models are built in the matter-dominated regime ($\sigma \ll 1$). This is the standard "fireball" shock model [23,136–140]. Magnetic fields are likely to be entrained in the ejecta. In the matter-dominated models, they are believed not to play a kinematically dominant role. As σ approaches and exceeds unity, magnetic fields become kinematically important. In such a magnetically-dominated jet, the ejecta would carry a globally ordered magnetic field. Notice that giving a same total outflow luminosity and at a same distance from the central engine, the absolute strength of magnetic fields does not vary significantly from $\sigma \lesssim 1$ to $\sigma \gg 1$. This is because the Poynting flux does not differ significantly, and different σ is mostly caused by different mass flux of the flow. Another comment is that due to magnetic acceleration and dissipation, σ

is expected to drop with radius [141–145]. As a result, one needs to specify a radius (from the central engine) when judging whether the flow is matter-dominated or magnetically-dominated.

Diagnosing the composition of GRB ejecta has not been an easy task. Although the $\sigma \ll 1$ models have been widely discussed mostly because of their simplicity, evidence that magnetic fields are playing an important role at least in some GRBs is gradually accumulating. (1) If $\sigma \geqslant 1$, an ordered magnetic field would give rise to strong linearly polarized synchrotron emission [146–149]. Strong linear polarization of gamma-ray emission has been claimed in some GRBs (e.g. [150,151]), although the results are subject to large uncertainty [152]. (2) Recent *Fermi* observations of GRB 080916C [85] revealed a series of nearly featureless Band-function spectra covering 6–7 orders of magnitude in energy throughout the entire burst. Such an observational fact brings challenge to the traditional fireball internal shock model. If the observed Band component is the non-thermal emission from internal shocks, one would expect a bright quasi-thermal spectral component from the fireball photosphere which outshines the non-thermal component, making the observed spectrum significantly deviated from the simple Band form. This led to the suggestion that the ejecta has to be Poynting flux dominated in order to suppress the bright photosphere thermal emission [153,154]. Since most *Fermi* LAT GRBs have Band-only spectra similar to GRB 080916C [155], one may speculate that most GRBs may function similar to GRB 080916C. The $\sigma \ll 1$ dissipative photosphere model (e.g. [156,157]) could give rise to a Band-like spectrum, but the model predictions cannot reproduce the broad spectra of GRB 080916C (e.g. [145,155] for detailed discussion). The *Fermi* LAT GRB 090902B [158] is a special case that shows bright quasi-thermal emission in the time-resolved spectra [159,155], which can be well interpreted as the photosphere emission [160]. The magnetization parameter σ is likely not very high, but the magnetic fields need to be strong in any case [160]. (3) As the ejecta is decelerated by the ambient medium, the existence and strength of the reverse shock depends on the GRB composition [161–164]. The general trend is the following [162]: when $\sigma \ll 1$, the reverse shock (RS) emission becomes progressively stronger as σ increases, because the synchrotron emission becomes progressively stronger in a stronger magnetic field. The RS brightness reaches the peak around $\sigma \sim 0.1$. When σ gets close and surpasses unity, the strong pressure from the magnetic field compensates part of the forward shock (FS) thermal pressure, so that the RS becomes progressively weaker until eventually disappears when the magnetic pressure can fully balance the FS pressure. Studying the strength of the RS can therefore diagnose ejecta composition. The bright optical flashes seen in several GRBs (e.g. GRBs 990123, 021211, 061126) require that the RS region is much more magnetized than the FS region, suggesting that the engine is carrying a strong magnetic field [165–168], with a σ close to (but does not exceed) unity. An early optical polarimetry observation of GRB 090102 revealed a $10 \pm 1\%$ polarization degree of emission during the early steep decay phase believed to be of the RS origin [169]. This suggests that the central engine ejecta carried an ordered magnetic field.

Besides the above observational diagnostics, claims about the GRB composition may be made using indirect theoretical modeling. For example, different models predict different radii of gamma-ray emission. The photosphere radius is typically $R_{\rm ph} \sim (10^{11}\text{–}10^{12})$ cm from the central engine. Internal shocks, on the other hand, occur at distances $R_{\rm IS} \sim \Gamma^2 c\delta t \sim 3 \times 10^{13}~{\rm cm}~\Gamma_{2.5}^2 \delta t_{-2}$, where δt is the typical variability time scale. Magnetic dissipation may occur in various radii. For models that invoke a striped-wind field geometry (relevant to pulsar-like central engines), significant magnetic dissipation can occur below the photosphere, so that the photosphere emission is enhanced. For models invoking helical magnetic geometry (relevant to black hole–torus engines), significant magnetic dissipation may not easy to occur at small radii, but rather occur at a large enough radius where the ordered field lines are distorted enough so that field lines with opposite orientations can approach each other and reconnect. Fast magnetic dissipation may be triggered either by collision-induced turbulent reconnection [145], by a switch from the collisional to the collisionless reconnection regimes [170], or by current instability [113]. In all these cases, the dissipation radius is usually larger than the photosphere radius, typically with $R_{\rm mag} \geqslant 10^{14}$ cm. Finally, for a neutron rich outflow, neutrons decay in all radii, but with a characteristic decay radius $R_n \sim 900c\Gamma = 2.7 \times 10^{15}~{\rm cm}~\Gamma_2$. Measuring the location of the MeV GRB emission $R_{\rm GRB}$ may shed light into the unknown composition of the GRB ejecta.

Observationally, it is not straightforward to measure $R_{\rm GRB}$ using the MeV data. Nonetheless, there are three indirect ways to infer this radius using X-ray, optical and GeV emission data: (1) *Swift* GRBs typically show a rapidly decaying early X-ray afterglow, which is found to be connected to prompt gamma-ray emission [171–173]. The leading interpretation is that this is the high-latitude emission of a conical jet after the prompt emission ceases abruptly [174,125,175,176]. Within this interpretation, the duration of the steep decay phase is defined by $\Delta t_{\rm steep} \sim (R_{\rm GRB}/c)(1-\cos\theta_j)(1+z) \sim (R_{\rm GRB}/c)(\theta_j^2/2)(1+z)$. For a typical jet angle $\theta_j \sim 0.1$, the data generally require that $R_{\rm GRB} \geqslant 10^{15}$ cm [177,178]; (2) Some GRBs have prompt optical emission detected roughly tracking gamma-ray emission [179,180]. If this optical emission is from the same emission region as gamma-rays, the GRB emission site can be constrained by requiring that the synchrotron self-absorption frequency is below the optical band. For the naked-eye GRB 080319B, this gives $R_{\rm GRB} \sim 10^{16}$ cm [180,181]. Constraints from other GRBs with prompt optical detections or upper limits give $R_{\rm GRB} \geqslant$ several $\times\, 10^{14}$ cm for typical GRB Lorentz factors [182]; (3) *Fermi* observations suggest that for a good fraction of GRBs, the MeV Band-function spectra extend to the GeV range, suggesting that GeV emission is from the same region as the MeV emission. For these bursts, the detected maximum GeV photon energy can be used to constrain $R_{\rm GRB}$ along with Γ [183]. For example, GRB 080916C gives a constraint $R_{\rm GRB} \geqslant 10^{15}$ cm in general [153], and $R_{\rm GRB} \sim 10^{16}$ cm if $R_{\rm GRB} \sim \Gamma^2 c\delta t$ is assumed [85]. A general picture emerging from these indirect constraints is that $R_{\rm GRB}$ is usually large, typically $\sim 10^{15}$ cm. This is also consistent with some model constraints based on MeV observations [184,185]. These large emission radii are consistent with the expectation of high-σ models, although low-σ models are not ruled out (but the parameter space is constrained). The caveat here is that the optical/GeV emission may not always be from the same region as MeV emission. For example, various arguments suggest that the gamma-ray emission radius may be smaller than that of optical emission in GRB 080319B [186–188]. The distinct GeV component of GRBs 090902B and 090510 is very likely from a different radius from the MeV component [86,158,155].

To summarize, the case of GRB composition is inconclusive. Evidence of a strongly magnetized central engine is accumulating, although the σ value in the GRB emission region is not well constrained. It is possible that σ may vary from burst to burst. This may sound unnatural. However, as explained above, when σ is greater than, say, 0.3, the increase in σ does not correspond to a further increase of Poynting flux, but rather corresponds to a decrease in the associated matter flux. As a result, a slight change in matter flux may result in a significant change in the σ value in the outflow (e.g. from $\sigma \lesssim 1$ to $\sigma \gg 1$). This is entirely possible. Since σ is a decreasing function of radius [141–145], one needs to specify a radius of reference for comparison in order to get a coherent picture of GRB magnetization. For example, it is possible that $\sigma \gg 1$ initially in the GRB emission region, σ is moderately high in the GRB emission region, and $\sigma \lesssim 1$ at the deceleration radius after the global magnetic dissipation process is over [145].

GRB composition is greatly tied to two interesting topics: whether GRBs are the dominant sources of ultra-high energy cosmic rays (UHECRs) [189,190] and high energy neutrinos [191–193]. These models all invoked a baryon-dominated outflow. If GRBs are on average Poynting-flux-dominated, the strengths of these signals would drop by a factor $(1+\sigma)^{-1}$, rendering GRBs not necessarily the dominant contributors to UHECRs and the high energy neutrino background.

2.5. Energy dissipation and particle acceleration mechanism

The main energy sources of a GRB include the gravitational accretion energy ($E_{\rm grav} \sim (1/2)GMm/R \sim 1.3 \times 10^{53}$ erg $\times$ $(M/10M_\odot)(m/1M_\odot)/R_7$, where M is the mass of the accretor and m is the mass of accreted materials) and the rotation energy of the central BH ($E_{\rm rot,BH} \sim M_{\rm BH}c^2[1-\sqrt{(1/2)(1+\sqrt{1-a^2})}] \leqslant 0.29M_{\rm BH}c^2 \sim 5.2 \times 10^{54}$ erg $(M_{\rm BH}/10M_\odot)$) or NS ($E_{\rm rot,NS} \sim (1/2)I\Omega^2 \sim 5 \times 10^{52}$ erg $I_{45}\Omega_4^2$). Besides, the central engine carries a magnetic field energy $E_{\rm mag} \sim (1/6)R^3B^2 \sim 1.7 \times 10^{50} B_{15}^2 R_7^3$. For quark star scenarios, an extra phase transition energy (of the same order of the accretion energy) may be added to the energy budget.

In a GRB, energy is transferred among various forms in different stages. A fraction of the gravitational potential energy is initially converted into thermal energy, forming a hot fireball of photons, electron/positron pairs and a small number of baryons. The fireball expands under its own thermal pressure, and converts thermal energy to the bulk kinetic energy of the ejecta. Torqued by magnetic fields, the spin energy of the central object can be converted into a Poynting flux, which is entrained in the ejecta. The ejecta can be also accelerated under the internal magnetic pressure of the ejecta.

At the photosphere radius, photons initially advected in the fireball are released, giving rise to a quasi-thermal spectrum (probably modified by Compton upscattering). This is the first location where photons are released. Above the photosphere, kinetic energy can be converted into particle energy and then into radiation in shocks. Alternatively, Poynting flux energy can be converted into particle energy and then into radiation in reconnection regions. These dissipation regions are additional sites to emit photons. The observed GRB emission is from one or more of these emission sites.

Shock dissipation is the widely discussed energy dissipation mechanism. The internal collisions within an unsteady matter-dominated wind injected from the central engine give rise to internal shocks [140,194]. The relative Lorentz factor between the two colliding shells can range from mildly relativistic ($\Gamma_{\rm rel} \gtrsim 1$) to relativistic ($\Gamma_{\rm rel} \sim$ a few to tens). After the collisions, it is assumed that shells merge. The leading fast shell interacts with the circumburst medium and drives an "external" forward shock into the medium [138,195]. A reverse shock propagates into the ejecta until crossing it [196–198]. The shocked materials between the forward and the reverse shocks form a "blastwave". The forward shock is initially relativistic. The reverse shock is mildly relativistic if the central engine duration is not long (the thin shell regime), but could be highly relativistic if the central engine duration is long enough (the thick shell regime) [199]. During the self-similar deceleration phase [200], the blastwave may be refreshed by slow ejecta lagging behind [201] or a Poynting flux injected by a long-lasting central engine (e.g. a spinning down millisecond pulsar or magnetar) [123,124].

Particles (both baryons and leptons) are believed to be accelerated in shocks. The well known process is the first-order Fermi acceleration. The effect is well known in the non-relativistic regime. For relativistic shocks, particle-in-cell (PIC) simulations are starting to unveil the acceleration details [202–204]. A power law tail develops as simulation time grows. A relativistic Maxwellian component is still observed in the current simulation, although it may be significantly eroded eventually [203]. Observationally there is no significant signature for such a relativistic Maxwellian component.

For a magnetized upstream, the shock jump condition is modified [205]. The energy that is available for dissipation is the matter part, which is $1/(1+\sigma)$ of the total energy [162]. Without magnetic dissipation, the magnetic energy in the flow (a portion of $\sigma/(1+\sigma)$) remains intact. For deceleration of a magnetized ejecta by an unmagnetized circumburst medium, the strength of the reverse shock progressively decreases [162,163] until completely disappears as σ increases to 10 s to ~ 100, when the forward shock internal pressure is no longer stronger than the magnetic pressure in the ejecta [162]. For collisions between two magnetized shells, a pair of shocks would propagate into both shells as long as the ram pressure exceeds the magnetic pressure of the shells. These shocks are weak, but in any case, would serve to distort the ordered magnetic field lines in the shell [162,145].

Whether and how particles are accelerated in magnetized shocks is subject to more investigations. PIC simulations [206] suggest that for a relativistic ($\Gamma \gtrsim 5$) magnetized ($\sigma > 0.03$) shock, particle acceleration is possible only within a narrow range of magnetic inclination angles ($\lesssim 34^\circ/\Gamma$). On the other hand, the reverse shock model to interpret early optical flashes require that the reverse shock is more magnetized than the forward shock (with σ close to 0.1) [166,165,167]. A $\sim 10\%$ linear polarization degree was measured in the early optical afterglow for GRB 090102 [169], which is consistent with emission from a magnetized reverse shock. The inconsistency between data constraints and PIC simulations may be partially alleviated by the following two factors: First, for thin shells the reverse shock invoked in GRB modeling is usually transrelativistic (i.e. reaching mildly relativistic at the end of shock crossing) [199]. So the allowed magnetic inclination angle space is much larger. Second, If the outflow was initially Poynting flux dominated, it must have gone through significant magnetic dissipation during the GRB prompt emission phase so that σ has dropped to around or below unity. Turbulence may have significantly distorted the ordered magnetic field configuration, so that during the deceleration phase, the magnetic field lines are no longer mostly perpendicular to the shock normal [145].

Besides shocks, magnetic dissipation is another effective way to accelerate relativistic particles. This is associated with reconnection of magnetic field lines with opposite polarity. The full details of reconnection is not well understood. The main difficulty has been that reconnection speed is slow in a steady state [207,208]. In the GRB context, continuous slow reconnection below and slightly above the photosphere may enhance photosphere emission, and lead to an up-scattered non-thermal tail above the photosphere thermal peak [209–211,157]. In order to produce bursty emission above photosphere to power the observed GRBs, the traditional Sweet–Parker reconnection speed is too low. A possibility is that reconnection proceeds via turbulence, so that multiple sites reconnect simultaneously [212]. For a high-σ flow, turbulence may be induced through multiple internal collisions which distort the ordered magnetic fields. A reconnection–turbulence cascade may result, which would discharge a significant fraction of magnetic energy to power a GRB with high radiative efficiency. This is the Internal Collision-induced MAgnetic Reconnection and Turbulence (ICMART) model of GRBs [145]. Particle acceleration in such turbulence–reconnection events is a difficult problem. Qualitatively, one can have three competing processes: direct electric field acceleration in current sheets, first-order Fermi acceleration between two approaching magnetic field lines, and the second-order Fermi acceleration in turbulence. Unfortunately, no currently available numerical tools can model the detailed particle acceleration processes in a relativistic, turbulent, dissipative, and strongly magnetized fluid. An alternative proposal for fast reconnection is the switch between collisional and collisionless regimes for a striped wind geometry [170]. It is interesting to further investigate how this proposal may account for the GRB prompt emission phenomenology.

Another particle acceleration mechanism in a strongly magnetized flow is the comoving Poynting flux acceleration [213], or inductive and electrostatic acceleration [214,215]. Particles "surf" on a wave of electric fields and gain energy. The applications of such a mechanism to GRBs have been discussed but are not explored in detail.

A dedicated review on particle acceleration in GRBs can be found in this issue [216].

2.6. Radiation mechanism

GRB prompt emission is characterized by a smoothly-joint broken-power-law named "Band" function [217]. The "non-thermal" nature of the spectrum demands that the emission is produced by a population of particles (likely leptons) with a power law energy distribution. The leading radiation mechanisms include synchrotron (or jitter) radiation, Synchrotron Self-Compton (SSC), and Compton upscattering of a thermal seed photon source. GRB afterglow has a broad-band spectrum at any epoch. The main contributor to afterglow emission is the synchrotron and SSC emission of the electrons accelerated in the external shock.

While the origin of the external shock afterglow is relatively well modeled (see Section 2.8 for further discussion), the radiation mechanism of the prompt GRB emission is subject to debate.

The leading mechanism is synchrotron radiation [218,219]. This is because it is the most naturally expected non-thermal emission mechanism. The GRB central engine is likely magnetized. Internal shocks can also generate magnetic fields through plasma instabilities [220,204]. Shock accelerated electrons must gyrate in the magnetic fields and radiate synchrotron photons.

The most straightforward synchrotron model, however, suffers a list of criticisms. (1) The synchrotron cooling time scale is typically much shorter than the dynamical time scale, so that electrons are in the "fast cooling" regime. The expected photon spectrum below E_p is supposed to have a photon index $\alpha = -1.5$, while the observations show a typical value of $\alpha \sim -1$. This is the fast cooling problem [221]. The possible solutions to this problem include introducing a rapidly decaying magnetic field in the internal shock region [222], introducing slow heating in the emission region (e.g. in an ICMART event) [145,223], and introducing Klein–Nishina cooling [224]. (2) The hardest low energy photon index is supposed to be $\alpha = -2/3$ in the synchrotron model (corresponding to the $F_\nu \propto \nu^{1/3}$ regime of synchrotron emission). However, a fraction of GRBs have α even harder than this "synchrotron line of death" [225]. Possible solutions include introducing contributions from the thermal photosphere [226], considering synchrotron self-absorption [227], and introducing "jitter" radiation [228]. (3) For typical parameters, the predicted E_p from synchrotron emission is about 2 orders of magnitude smaller than the observed value. This requires that only a small fraction of electrons are accelerated in the internal shocks [229,230]. The same requirement is needed to correctly derive the synchrotron self-absorption frequency in internal shocks [182]. In a high-σ flow, this problem is naturally solved [145]. (4) Within the internal shock model, it is argued that the allowed parameter regime for synchrotron model is greatly constrained [185]. Such a limitation applies to the internal shock model. For magnetic dissipation synchrotron models such as the ICMART model [145], the constraint is much weaker.

A variant of the synchrotron radiation mechanism is the jitter radiation mechanism [228]. Within this scenario, magnetic fields have too small a coherence length λ_B so that electrons cannot make a complete gyration. The typical jitter emission frequency no longer depends on the strength of the magnetic field, but is related to λ_B. The low energy photon index below E_p can range from 0 to -1 [231]. One issue of this scenario is that the assumed small coherence scale is not revealed from PIC numerical simulations of relativistic shocks [232]. On the other hand, such a small coherence scale may be realized in magnetic reconnection regions [233], so that the radiation mechanism may be relevant in models that invoke magnetic dissipation as the origin of GRB emission.

The second radiation mechanism candidate to interpret prompt GRBs is SSC. Within this scenario, the synchrotron radiation peaks in the IR/optical/UV range, and the observed GRBs are dominated by the SSC emission [234]. It was found that within the internal shock model, the allowed parameter space of SSC is much larger than that of synchrotron if all the electrons are accelerated [185]. Introducing an assumption that only a small fraction of electrons are accelerated would largely alleviate this problem [235]. The SSC mechanism attracted serious attention following the discovery of the "naked-eye" GRB 080319B [180]. Bright optical pulses are found associated with gamma-ray pulses, with flux greatly exceeding the extrapolation of gamma-ray emission into the optical band. An immediate possibility is that optical is due to synchrotron radiation, while gamma-rays are due to SSC [181,180,236]. Counterarguments against the simplest SSC mechanism for GRB 080319B include the energy crisis (since $Y \sim 10$, the second-order IC component would be even more energetic) [237,187, 238], ~ 1 s lag of the optical emission with respect to the gamma-ray emission [239], and the difficulty of interpreting the more variable gamma-ray lightcurve (than optical) [188]. More complicated SSC models invoking turbulence in the emission region may overcome some of these criticisms [236].

The third radiation mechanism commonly discussed in the literature is Compton upscattering of thermal photons. The leading scenario is upscattering off thermal photons from the jet photosphere [209,210,240,241,211,242,156,157,243]. This requires energy dissipation below and slightly above the photosphere. Within this scenario, the observed E_p is essentially the temperature of the photosphere. Upscattering naturally gives rise to a power law spectrum above E_p. The spectral index below E_p, is however difficult to alter from the Rayleigh–Jeans slope (corresponding to $\alpha = +1$ rather than $\alpha = -1$ as typically observed). Considering sub-photosphere heating and equal-arrival-time effect in a relativistic ejecta, one gets $\alpha \sim 0.4$ [156], still much harder than the observed spectrum. The equal arrival time effect would modify α to approach -1 at late times when the flux already drops significantly [243]. This may be relevant when the central engine activity is over, but is not applicable during the prompt emission phase when a continuous wind is ejected from the central engine. In general, the dissipative photosphere models have the difficulty to interpret the low energy photon spectral index of GRBs.

Besides the photosphere, other thermal sources can give rise to seed photons for relativistic electrons to up-scatter. These photon sources include the thermal photons released from the exploding star [244], the thermal photon "glory" from the progenitor star that is trapped by the environment [245], as well as thermal photons from shock breakout [246].

Finally, hadronic mechanisms (proton synchrotron and proton–photon interaction to produce charged and/or neutral pions) have been also suggested to interpret prompt GRB emission (e.g. [247–249]). Since protons are radiatively inefficient as compared with leptons, these models require that protons carry most of the total energy (i.e. proton dominated).

It is difficult to identify the correct radiation mechanism with the current available data. The "smoking gun" would be the gamma-ray polarization data. Although both synchrotron radiation in an ordered magnetic fields [113,148] and IC viewed at certain angles [250,251] can give high degree of polarization, systematically studying the statistical polarization properties of a sample of GRBs can differentiate the competing models and may lead to identification of the radiation mechanism of GRB prompt emission [149].

A dedicated review on multiwavelength GRB prompt emission observations can be found in this issue [252].

2.7. Long term central engine activity

One of the major discoveries of *Swift* is that the so-called "afterglow" is not only the emission from the external shock (as generally believed in the pre-*Swift* era), but also includes emission from a long-lasting central engine. The arguments for a long lasting central engine lie in the following three pieces of evidence.

The most convincing evidence is the existence of X-ray flares following nearly half of *Swift* GRBs [253–255]. These flares have sharp rise and sharp decay. The morphology is essentially impossible to be interpreted within the framework of the external shock model [256]. One therefore needs to appeal to late central engine activities to interpret them [253,125,257–259]. The most convincing evidence of such an interpretation is the reset of the clock for each episode of engine activity, as is suggested from the data: in order to interpret the decay following an X-ray flare as the high latitude emission effect, the required T_0 is usually right before the rise of the flare [175]. Such a property cannot be naturally interpreted within other X-ray flare models that do not invoke late central engine activities (e.g. [260]).

Next, a small fraction of GRB X-ray afterglows show an extended plateau followed by a sudden drop of flux with a decay index steeper than 3 (sometimes even as steep as 9) [128–130]. Such a rapid fall cannot be interpreted within the external shock models, and needs to invoke internal dissipation of a long lasting central engine wind. Such a plateau is therefore sometimes also called an "internal plateau" [129,130]. For comparison, most X-ray afterglow lightcurves show a plateau followed by a "normal" decay with slope ~ -1 [125,126]. Within the external shock interpretation, the X-ray plateaus are due to adding energy into the blastwave. Before observing the internal plateaus, there have been two possibilities to account for such a refreshed shock: a long lasting central engine [123,124] or piling up slow materials ejected promptly [201,261].

With the discovery of internal plateaus, it is now clear that some GRBs indeed have a long-lasting central engine activity, so that the former scenario can operate at least in some GRBs.

Last, some authors even interpret the most common X-ray plateaus (those followed by a t^{-1} normal decay phase) as emission from the central engine [262–265]. The main reason is that in more than half cases, no optical break was discovered at the transition time from the plateau to the normal decay phase [266,129], and that there is essentially no spectral evolution across the temporal break [267]. Such a chromatic behavior is very difficult to interpret within the framework of the external shock models. Invoking two-component external shock jets [268] would require contrived shock parameters and unnatural assumptions. Invoking a long lasting reverse shock [269,270] would require that the forward shock emission is suppressed by many orders of magnitude. Another possibility, i.e. dust scattering effect [271], can interpret the lightcurve but not the spectral evolution as observed for most GRBs [272]. One therefore is left with the possibility that the X-ray emission is dominated by the internal emission of a long-lasting central engine. Indeed, a quantitative X-ray afterglow model attributing X-ray emission to the dissipative photosphere of a long lasting central engine wind can reproduce the shallow, normal, and late break of X-ray lightcurve with chromatic features as observed [273].

To conclude, the observational data demand the following two aspects related to the GRB central engine. First, the engine is usually still active after the prompt emission phase is over, and can last up to $> 10^4$ s after the trigger. Second, there can be two types of central engine activities, an erratic component that can power X-ray flares, and a smooth component that can power the plateaus (those followed by a steep decay segment or even those followed by a normal decay segment).

There is no well accepted mechanism yet to account for the erratic behavior of the late central engine activities. Nonetheless, some ideas have been proposed. These include fragmentation of the collapsing star [274], fragmentation of the accretion disk of both massive star and compact star GRBs [275], intermittent accretion behavior caused by a time variable magnetic barrier [276], magnetic bubbles launched in a post-merger differentially rotating, proto-neutron star [277], helium synthesis in the post-merger debris of a compact star GRB [278], and quakes in solid quark stars [120]. In any case, since the neutrino-driven jet luminosity drops steeply when the accretion rate becomes small [279], the existence of low-luminosity X-ray flares at late times demand that the late jets that power X-ray flares are driven and collimated by magnetic mechanisms [281]. Another caveat is that an intermittent jet may not always correspond to intermittent accretion. It may be possible that accretion is continuous, but another mechanism (e.g. magnetic activity) is responsible for the observed intermittent jet emission (e.g. [280]).

The mechanisms to account for a long-lasting continuous late central engine activity include fall-back accretion onto the black hole engine [282–284], or tapping the spin energy of a strongly magnetized millisecond pulsar [123,124]. For the latter possibility, one needs to interpret the energetic prompt gamma-ray emission without introducing a black hole–torus central engine. Possible mechanisms include hyperaccretion onto a neutron star [106] or phase transition into a quark star [116–119].

To firmly test the long-lasting central engine scenarios, additional observational channels are needed. For example, X-ray polarization measurements for X-ray flares would be essential to test the magnetic nature of the late jet [281]. Gravitational wave observations during the plateau phase would shed light onto the nature of the millisecond pulsar central engine [285].

2.8. External shock afterglow physics

Among all the topics discussed in this review, the external shock afterglow physics is the most definite one. Even though the forward shock afterglow model has some free parameters,[2] the dynamics of the blastwave, the radiation spectrum at any instant, as well as the lightcurve at any wavelength can be uniquely predicted once these input parameters are specified [196,286–288]. As a result, using multi-band (radio, optical and X-rays) data, one can constrain these unknown parameters based on the model [289–292]. More complicated factors, such as jet break [293,294], energy injection into the blastwave [201,123,124,295], angular structure of the jet [296–298,167,180], as well as transition to the non-relativistic phase [299, 300] can be added into the model to interpret more complicated observational behaviors.

Modeling afterglow using the external shock model has been the main topic before *Swift*. *Swift* observations of early afterglows on the other hand revealed a more complicated picture. The X-ray afterglows show a canonical lightcurve with 5 distinct components [125,126]. The early steep decay component connecting the prompt emission [171–173] (Component I of [125]) and the erratic X-ray flares (Component V of [125]) are believed to be of the internal origin. The rest three segments: shallow decay (II), normal decay (III) and the late steep decay (IV) are well interpreted within the external shock model: II is the external shock during the continuous energy injection phase, III is the external shock emission after injection is over, and IV is the external shock emission after the jet break phase [125,126,301]. According to such an interpretation, the two breaks are hydrodynamical breaks and should also appear in other wavelengths as well (i.e. achromatic). This was indeed seen in some GRBs (e.g. GRB 060729 and GRB 060614 [302,303]). However, chromatic behaviors were discovered around both breaks in a good fraction of GRBs [266,129,90]. This suggests that the X-ray afterglow might not be always of the external shock origin. Therefore, in the *Swift* era, the afterglow modeling made one step backwards: instead of

[2] For the standard model, five parameters are needed: the total energy of the blastwave $E_{\rm iso}$, one parameter to describe the circumburst medium – the number density n for a constant ISM model, or the $A_\star$ parameter for the stellar wind model, one parameter for electron energy distribution p, and two parameters for shock energy partition – the electron equipartition parameter $\epsilon_{\rm e}$ and the magnetic field equipartition parameter $\epsilon_{\rm B}$.

constraining the afterglow model parameters using the data, one needs first to identify which emission component is from the external forward shock, and which is not.

An important result from the pre-*Swift* era was that massive star (Type II) GRBs are collimated, and the jet opening angles are such distributed that the jet corrected energy is roughly constant [88,89,304]. *Swift* observations raise cautions to accept this conclusion readily. There is no platinum jet breaks identified (i.e. those clearly show achromatic feature in all wavelengths) [90]. Some bursts have chromatic breaks at the so-called "jet break" epoch, while some bursts do not have a break at much late epochs [90,91]. More late time optical observations (e.g. [305]) are needed to reveal jet breaks and GRB collimation and energetics.

Another important aspect of the external shock afterglow physics is the emission of the reverse shock that propagates into the ejecta. Traditionally the ejecta is approximated as a finite width shell with uniform density. The reverse shock therefore gives a short-live emission signature. Since the density of the shell is approximately Γ times of that of the medium, and since the FS and RS regions share roughly the same pressure and internal energy, each electron in the RS region has less energy than those in the FS, so that the peak synchrotron frequency is smaller by roughly Γ^2. As a result, while the FS emission initially peaks in X-rays and above, RS emission peaks in IR/optical/UV [196–198]. At the shock crossing time, the synchrotron emission peak fluxes, typical frequencies between RS and FS are connected through some simple relations [306,166]. For typical shock parameters for both the FS and the RS, the RS emission is not expected to be very bright. The optical lightcurve is characterized by double peaks, the first RS peak marking fireball deceleration, and the second FS peak related to crossing of the typical synchrotron frequency in the optical band [166]. The bright optical flashes characterized by a $F_\nu \propto t^{-2}$ decay followed by a normal $F_\nu \propto t^{-1}$ decay (e.g. [307]) requires that the RS is more magnetized than the FS [166,168]. There is also a regime where the typical RS synchrotron frequency is way below the optical band, so that there is essentially no RS signature in the optical lightcurve [308]. Considering ejecta magnetization, the RS flux increases initially as σ increases from below, but would start to decrease as σ approaches unity and gradually diminishes when $\sigma \gg 1$ [162,163]. A group of GRBs are found to have a smooth afterglow onset bump dominated by the emission from the FS (e.g. [84]). These either have a low RS typical frequency [308] or have a highly magnetized ejecta at the deceleration time [162,163].

For a wind medium, the RS is usually relativistic, which is accompanied by a prominent optical emission signature [309, 310]. SSC in the RS region [311] or cross IC between the electrons and photons from FS and RS [312,313] could be important when the RS emission is prominent, which may contribute to early X-ray and gamma-ray afterglow emission.

It is possible that the ejecta do not have a uniform Lorentz factor, luminosity and density. Considering an ejecta with a more complicated stratification profile, the RS emission lightcurve can be made to have rich features, including reproducing the canonical X-ray lightcurve as observed by *Swift* [269,270]. However, for nominal parameters, the FS emission is brighter by several orders of magnitude. In order to interpret the data with the RS model, one has to argue that the FS emission is suppressed [269,270].

A dedicated review on GRB afterglow can be also found in this issue [314].

2.9. Origin of high energy emission

Before *Fermi*, emission above 100 MeV was detected only in a handful of GRBs (e.g. [315,316]). The Large Area Telescope (LAT) on board *Fermi* makes it possible to detect high energy emission from GRBs regularly. Although somewhat lower than the pre-launch predictions, the current detection rate of ~ 9 per year allows collection of a moderate sample of GRBs with detected emission above 100 MeV [85–87,158,155]. A dedicated review on *Fermi* LAT GRB science can be also found in this issue [317].

The properties of GRB high energy emission can be summarized as follows (e.g. [155] for a comprehensive study): (1) The LAT band emission is found delayed with respect to the GBM band emission in several (but not all) GRBs [85,86,158,155]. (2) Among 17 LAT GRBs detected before May 2010, 14 have time-resolved spectra consistent with being a single Band function extending to both low energy and high energy regimes [155]. An example is GRB 080916C [85], which shows a featureless Band function covering 6–7 orders of magnitude. The Band function parameters (the low- and high-energy photon indices α and β and peak energy E_p) do not vary significantly as the time resolution becomes progressively smaller. This suggests that the Band function may not be a superposition of many more elemental spectral components (e.g. blackbody), but is an elemental spectral component of its own [155]. (3) Three GRBs have at least two spectral components in the time resolved spectra. GRB 090510 and GRB 090902B have an extra power law component extending to high energies [86,158,155]. GRB 090926A may have an extra spectral component setting in after ~ 11 s, which may have a high energy spectral cutoff [318]. (4) The MeV component of GRB 090902B is likely of the thermal origin. The time integrated spectrum is a narrow Band function plus a power law. As the time bin becomes progressively smaller, the time-resolved spectra of the MeV component become progressively narrower [155], so that it can be fit with a multi-color blackbody function [159] or a blackbody function [155] (with the superposition with a power law component). The MeV component of GRB 090510 can be fit as a power law with an exponential cutoff [86,155], which may have a similar origin as the MeV component of GRB 090902B. (5) Overall, there might be three elemental spectral components in the prompt GRB spectra [155]: a Band component (Band), a thermal-like component (BB), and an extra power law component with a possible cutoff at high energies above the LAT band (PL). The observed GRB spectra may be decomposed of one or more of these elemental components. Current observed combinations include Band only (e.g. GRB 080916C), BB + PL (e.g. GRB 090902B), and probably Band +

PL (e.g. GRB 090926A). Other possible combinations include Band + BB and Band + BB + PL, which exist in some GRBs and may be tested with future bursts. (6) During the prompt emission phase (defined by GBM-band emission), high energy photons are usually found to track the MeV photons in time. This not only is valid for the Band-only GRBs such as GRB 080916C, but also applies to GRBs showing a distinct spectral component at high energy (e.g. GRB 090902B) [155]. This hints that during the prompt emission phase, the high energy photons are likely of an internal origin. (7) Puzzlingly, the > 100 MeV photons decay more slowly than the MeV photons. After the GBM-band burst is over, LAT-band photons are usually observed to decay with a single power law with a slope ~ -1.4 [319,155]. This suggests either that the entire high energy emission has a different origin from the MeV emission (which is in contrast with the points 2 and 6 above) [322,323,319], or that the high energy lightcurve is the superposition of two components with a second (external shock) component setting in as the prompt emission fades [155,320].

Even though the origin of high energy emission is still subject to debate, these new data shed light into several open questions in GRB prompt emission physics (e.g. topics discussed in Sections 2.4–2.6). (1) The featureless Band-only GRBs such as GRB 080916C are difficult to interpret within the simplest baryonic fireball picture. If the entire non-thermal spectrum is from the internal shocks, then the photosphere emission of the hot fireball is expected to be bright enough to show up above the detected Band spectrum [153,154]. This led to the suggestion that GRB 080916C and most LAT GRBs have $\sigma \gg 1$ at the central engine, and probably also in the emission region as well [153]. The bright thermal emission of GRB 090902B, on the other hand, point towards a fireball picture [160], with $\sigma \lesssim 1$. This would suggest a diverse composition among GRBs. The possibility that the Band spectrum is from a dissipative photosphere has been discussed (e.g. [321,156, 157]). These models have specific predictions that are not consistent with the data. For example, the predicted spectrum cannot extend to energies higher than ~ 1 GeV, while the Band spectra extend all the way to rest-frame ~ 70 GeV for GRB 080916C. The assumption that this prompt GeV emission is from the external shock is not supported by detailed data analysis [155]. Also the low energy photon index of a dissipative photosphere is predicted to be $\alpha \sim 0.4$, which is much harder than the observed $\alpha \sim -1$. (2) The long-term GeV emission may be originated from the external shock. This requires some extreme parameters for the external shock [322,323], a radiative blastwave [319] or a Klein–Nishina cooling dominated shock [325,326]. GeV emission during the prompt emission phase, however, is not easy to interpret within the external shock model [327,328,320], and is likely of an internal origin, as suggested by the data [155]. (3) The delayed onset of GeV emission has been interpreted as emergence of the upscattered cocoon emission [324], synchrotron emission from shock accelerated protons [249], delayed residual internal shock emission [329], as well as the delayed fireball acceleration to an extremely high Lorentz factor [330]. Alternatively, it can be simply due to change of particle acceleration condition or pair production opacity during the early stage of a GRB [145,155].

Bright GRBs co-detected by *Fermi*/LAT and *Swift* would be highly valuable to understand the nature of high energy emission. This is because a *Swift* BAT trigger would lead to early XRT and UVOT observations. Some GeV models (e.g. the external shock model) have specific predictions in the X-ray and UV/optical band. The detections of early afterglows by *Swift* would prove or disprove these predictions, so that one can narrow down the allowed models for GRB high energy emission. Unfortunately, the chance of LAT/*Swift* joint trigger is low. The only case so far (GRB 090510) was a short GRB [331]. More cases, especially for long GRBs, are highly desirable.

2.10. Cosmological setting

GRBs are cosmological events. The redshift distribution of GRBs spans from $z = 0.0085$ (for GRB 980425 [11]) to $z = 8.2$ (for GRB 090423 [32,33]). Several open questions of GRBs within the cosmological context include the following:

Are massive star GRBs good tracers of star formation history of the universe? Do these GRBs favor a low metallicity environment? Does the GRB luminosity function evolve with time? These questions are related to each other. In order to account for the detections of GRB 080916 at $z = 6.7$ [34] and GRB 090423 at $z = 8.2$ [32,33], the GRB event rate at high-z should be higher than the simple extrapolation of the known star formation history (e.g. [332]) to higher redshifts [333,33]. One possibility is that GRBs still follow the star formation history of the universe, but there is a rise of SFR at high z due to the contribution from the population III stars [334]. Although the high-z GRB excess may be interpreted this way, the fact that the observed high-z GRBs are not different from their nearby sisters [32,33] suggest that this factor is not adequate to interpret the current data. One therefore needs to argue that GRBs favor low metallicity environment [54,335–337] or their luminosity function evolves with redshift so that luminosity is higher at higher-z. These two effects are coupled with each other, and may not be differentiated with the L–z and $\log N$–$\log P$ data [337,336]. On the other hand, the low metallicity possibility is favored by the host galaxy modeling as well (e.g. [53,338,55]).

Can high-z GRBs probe the reionization history of the universe? The universe is known to be re-ionized around $z \sim 6$. The details of the reionization history is not well constrained (e.g. [339]). GRBs are believed to exist at as early as $z \sim 20$. As bright beacons in the “dark ages”, these high-z GRBs can probe the cosmic reionization history in their near IR afterglow spectrum. In particular, the damping wing bluewards of the Lyman-α “Gunn–Peterson” trough carries the information of the neutral hydrogen column density along the line of sight. This can in principle extend the intergalactic medium (IGM) ionization state mapping (previously by quasars [340]) to higher z's. One issue is that the GRB host damped Lyman-α (DLA) system would contribute to the observed neutral column, so that the IGM absorption feature is not clean (e.g. [341]). Numerical simulations suggest that the GRB host DLA column decreases with redshift [342,343]. Such a feature makes it more promising to use GRBs to probe reionization at $z > 8$. Since afterglow is rapidly fading, very early IR observations for high-z GRBs are needed to make breakthrough in this direction.

Do high-z GRBs have a different progenitor from the low-z ones? The first generation stars may be more massive than the nearby massive stars [344]. If these massive stars produce GRBs, they should be powered by supermassive black holes through the Blandford–Znajek mechanism [345,346]. These GRBs should be more powerful than normal GRBs. No such energetic high-z GRBs have been detected so far. On the other hand, recent numerical simulations revealed that the halo to form first generation stars may fragment, so that the first generation stars may be in binary systems with smaller masses [347]. The GRBs in such systems may be then not much different from the normal GRBs.

Observationally, the two highest-z GRBs (080916 and 090423) both have a rest-frame duration shorter than 2 s. One possibility is that this is due to a selection effect (i.e. the fainter pulses are buried below the noises). However, if the effect is intrinsic, one would wonder whether they are massive star (Type II) GRBs or compact star (Type I) GRBs (e.g. [31] and references therein). Applying the multiple criteria besides the duration and hardness information, it is highly likely that these bursts are Type II GRBs [31]. Under certain conditions (e.g. slow rotators), it is possible that a massive star only has a small torus after prompt collapse, so that a short duration GRB can be powered [348,349]. If future high-z GRBs prefer short durations, one then needs to seriously address why the conditions for a short accretion time are preferred for high-z massive stars.

A dedicated discussion on GRBs as cosmological probes can be also found in this issue [350].

3. The SVOM connection

The Chinese–French mission SVOM is a multi-wavelength GRB observatory scheduled to launch in 2014–2015 [5]. It carries four space-flown instruments: a wide field X-ray/soft γ-ray (4–250 keV) detector ECLAIRs, a hard gamma-ray (50 keV–5 MeV) detector GRM, a visible telescope VT, and an X-ray telescope MXT. A set of three ground based dedicated instruments, including two robotic telescopes (GFTs) and one wide angle optical monitor (GWAC), will complement the space borne instruments. Its operation window overlaps with that of *Fermi* and *Swift* and probably overlaps with other planned GRB missions (such as JANUS, EXIST) as well. After 2014–2015, several multi-messenger detectors (e.g. neutrino detector Icecube and gravitational wave detector Advanced LIGO) will be fully operating. It is foreseen that an exciting era of GRB study will be ushered in.

It is unrealistic to solve all the open questions discussed in this review, but some aspects of the problems will be better addressed for sure in the SVOM era. Here I discuss some prospects.

– **Classification & progenitor:** ECLAIRs and GRM can give independent T_{90} measurements for many GRBs. This will give a large sample to study energy-dependent T_{90} classification. Similar to *Swift*, SVOM will lead broad-band follow-up observations for many GRBs. This will allow collection of multi-criteria needed to diagnose the physical origin of the GRBs (e.g. [31]). SVOM will continue to study massive star (Type II) GRBs and compact star (Type I) GRBs to allow better understanding of their progenitors. SVOM is not ideal to detect standard short GRBs, but the sensitivity of ECLAIRs to soft X-rays would help to detect more cases of "extended emission" of short GRBs. This would offer a chance to study the condition of extended emission, as well as whether short GRBs with extended emission are different from the canonical short GRBs. SVOM will also be powerful to study nearby low-luminosity long GRBs, allowing a better statistics for these events, addressing their supernova associations, event rate, luminosity function, as well as whether they indeed form a distinct population from canonical GRBs.
– **GRB prompt emission physics:** ECLAIRs and GRM cover a different spectral window from *Fermi* GBM and LAT. The joint spectral analysis between the two instruments would allow diagnose of the prompt GRB emission spectral components (e.g. [155]). In particular, it allows a systematic analysis of the X-ray excess in the spectrum, addressing the existence/strength of the photosphere thermal emission component, shedding light into jet composition, energy dissipation, particle acceleration and radiation mechanisms. GWAC will also regularly monitor prompt optical emission. Detections or upper limits of optical emission during the prompt phase would lead to the constraint on the broad-band prompt spectrum, and therefore nail down the radiation mechanism (e.g. synchrotron vs. SSC) of the prompt GRB emission.
– **Afterglow and "foreglow" physics:** VT will regularly record early optical afterglow emission from GRBs. Being redder and deeper than *Swift* UVOT, VT is ideal to address the early optical emission physics, including categorizing the early afterglow behavior and addressing the origin of optically dark GRBs. Together with MXT, VT can address chromatic/achromatic behaviors (for temporal breaks and flares) between the two energy bands. This would allow a systematic study of the long-term central engine activity of GRBs. GWAC will be monitoring the SVOM field of view during and even before the GRB trigger. This provides a chance of studying prompt optical emission and leading to detection of upper limits of optical emission before the prompt emission. In view of the recent motivation of discussing GRB "prior emission" (e.g. [351,352]), both positive and negative detections of these "foreglows" would shed light onto the function of the GRB central engine.
– **Cosmological setting:** Having a softer bandpass than *Swift*/BAT, ECLAIRs may be able to detect more soft high-z GRBs. Deep upper limits of VT below 0.95 μm would promptly provide good GRB candidates with $z > 6$. So ideally SVOM would lead to more detections and identifications of high-z GRBs, offering the opportunity to better address high-z star

formation history, metallicity effect, GRB evolution, cosmic reionization, as well as whether population III stars could give rise to GRBs.

Acknowledgements

I acknowledge extensive discussion on the SVOM science with Jian-Yan Wei, Yu-Lei Qiu, Jin-Song Deng, and other members of the Chinese SVOM team, as well as with Frederic Daigne, En-Wei Liang, and Bin-Bin Zhang. I also thank Peter Mészáros and two referees for helpful comments. This work is supported by NSF through grant AST-0908362, and by NASA through grants NNX10AD48G, NNX09AT66G, NNX10AP53G, and NNX08AE57A.

References

[1] P. Mészáros, Gamma-ray bursts, Rep. Prog. Phys. 69 (2006) 2259–2322.
[2] B. Zhang, Gamma-ray bursts in the Swift era, Chinese J. Astron. Astrophys. 7 (2007) 1–50.
[3] N. Gehrels, E. Ramirez-Ruiz, D.B. Fox, Gamma-ray bursts in the Swift era, Annu. Rev. Astron. Astrophys. 47 (2009) 567–617.
[4] P.F. Michelson, W.B. Atwood, S. Ritz, Fermi gamma-ray space telescope: high-energy results from the first year, Rep. Prog. Phys. 73 (7) (2010) 074901.
[5] J. Paul, J. Wei, S. Basa, S.N. Zhang, The Chinese–French SVOM mission for gamma-ray burst studies, C. R. Physique 12 (2011) 298–308 (this issue).
[6] J. Greiner, A. Rau, The multiwavelength context in 2015 and beyond, C. R. Physique 12 (2011) 226–233 (this issue);
J. Greiner, A. Rau, Fermi gamma-ray space telescope: high-energy results from the first year, Rep. Prog. Phys. 73 (7) (2010) 074901.
[7] C. Kouveliotou, et al., Identification of two classes of gamma-ray bursts, Astrophys. J. 413 (1993) L101–L104.
[8] T. Sakamoto, et al., The second Swift BAT gamma-ray burst catalog, Astrophys. J. (2011), submitted for publication.
[9] J.P. Norris, J.T. Bonnell, Short gamma-ray bursts with extended emission, Astrophys. J. 643 (2006) 266–275.
[10] I. Horváth, et al., Detailed classification of Swift's gamma-ray bursts, Astrophys. J. 713 (2010) 552–557.
[11] T.J. Galama, et al., An unusual supernova in the error box of the γ-ray burst of 25 April 1998, Nature 395 (1998) 670–672.
[12] J. Hjorth, et al., A very energetic supernova associated with the γ-ray burst of 29 March 2003, Nature 423 (2003) 847–850.
[13] K.Z. Stanek, et al., Spectroscopic discovery of the supernova 2003dh associated with GRB 030329, Astrophys. J. 591 (2003) L17–L20.
[14] S. Campana, et al., The association of GRB 060218 with a supernova and the evolution of the shock wave, Nature 442 (2006) 1008–1010.
[15] E. Pian, et al., An optical supernova associated with the X-ray flash XRF 060218, Nature 442 (2006) 1011–1013.
[16] A.S. Fruchter, et al., Long γ-ray bursts and core-collapse supernovae have different environments, Nature 441 (2006) 463–468.
[17] S.E. Woosley, Gamma-ray bursts from stellar mass accretion disks around black holes, Astrophys. J. 405 (1993) 273–277.
[18] B. Paczýnski, Are gamma-ray bursts in star-forming regions?, Astrophys. J. 494 (1998) L45–L48.
[19] N. Gehrels, et al., A short γ-ray burst apparently associated with an elliptical galaxy at redshift $z = 0.225$, Nature 437 (2005) 851–854.
[20] D.B. Fox, et al., The afterglow of GRB 050709 and the nature of the short-hard γ-ray bursts, Nature 437 (2005) 845–850.
[21] S.D. Barthelmy, et al., An origin for short γ-ray bursts unassociated with current star formation, Nature 438 (2005) 994–996.
[22] E. Berger, et al., Afterglows, redshifts, and properties of Swift gamma-ray bursts, Astrophys. J. 634 (2005) 501–508.
[23] B. Paczýnski, Gamma-ray bursters at cosmological distances, Astrophys. J. 308 (1986) L43–L46.
[24] D. Eichler, et al., Nucleosynthesis, neutrino bursts and gamma-rays from coalescing neutron stars, Nature 340 (1989) 126–128.
[25] R. Narayan, B. Paczynski, T. Piran, Gamma-ray bursts as the death throes of massive binary stars, Astrophys. J. 395 (1992) L83–L86.
[26] N. Gehrels, et al., A new γ-ray burst classification scheme from GRB060614, Nature 444 (2006) 1044–1046.
[27] A. Gal-Yam, et al., A novel explosive process is required for the γ-ray burst GRB 060614, Nature 444 (2006) 1053–1055.
[28] J.P.U. Fynbo, et al., No supernovae associated with two long-duration γ-ray bursts, Nature 444 (2006) 1047–1049.
[29] M. Della Valle, et al., An enigmatic long-lasting γ-ray burst not accompanied by a bright supernova, Nature 444 (2006) 1050–1052.
[30] B. Zhang, et al., Making a short gamma-ray burst from a long one: Implications for the nature of GRB 060614, Astrophys. J. 655 (2007) L25–L28.
[31] B. Zhang, et al., Discerning the physical origins of cosmological gamma-ray bursts based on multiple observational criteria: The cases of $z = 6.7$ GRB 080913, $z = 8.2$ GRB 090423, and some short/hard GRBs, Astrophys. J. 703 (2009) 1696–1724.
[32] N.R. Tanvir, et al., A γ-ray burst at a redshift of $z \sim 8.2$, Nature 461 (2009) 1254–1257.
[33] R. Salvaterra, et al., GRB090423 at a redshift of $z \sim 8.1$, Nature 461 (2009) 1258–1260.
[34] J. Greiner, et al., GRB 080913 at redshift 6.7, Astrophys. J. 693 (2009) 1610–1620.
[35] E.M. Levesque, et al., GRB090426: the environment of a rest-frame 0.35-s gamma-ray burst at a redshift of 2.609, Month. Not. Roy. Astron. Soc. 401 (2010) 963–972.
[36] L.A. Antonelli, et al., GRB 090426: the farthest short gamma-ray burst?, Astron. Astrophys. 507 (2009) L45–L48.
[37] L.-P. Xin, et al., Probing the nature of high-z short GRB 090426 with its early optical and X-ray afterglows, Month. Not. Roy. Astron. Soc. 410 (2011) 27–32.
[38] J.S. Bloom, N.R. Butler, D.A. Perley, Gamma-ray bursts, classified physically, in: M. Galassi, D. Palmer, E. Fenimore (Eds.), American Institute of Physics Conference Series, vol. 1000, 2008, pp. 11–15.
[39] T.Q. Donaghy, et al., HETE-2 localizations and observations of four short gamma-ray bursts: GRBs 010326B, 040802, 051211 and 060121, arXiv:astro-ph/0605570, 2006.
[40] D.A. Kann, et al., The afterglows of Swift-era gamma-ray bursts. I. Comparing pre-Swift and Swift-era long/soft (type II) GRB optical afterglows, Astrophys. J. 720 (2010) 1513–1558.
[41] D.A. Kann, et al., The afterglows of Swift-era gamma-ray bursts. II. Short/hard (type I) vs. long/soft (type II) optical afterglows, Astrophys. J. (2011), in press, arXiv:0804.1959.
[42] H.-J. Lü, E.-W. Liang, B.-B. Zhang, B. Zhang, A new classification method for gamma-ray bursts, Astrophys. J. 725 (2010) 1965–1970.
[43] R.L.C. Starling, et al., Discovery of the nearby long, soft GRB 100316D with an associated supernova, Month. Not. Roy. Astron. Soc. 411 (2011) 2792–2803, doi:10.1111/j.1365-2966.2010.17879.x, arXiv:1004.2919.
[44] S. Savaglio, K. Glazebrook, D. Le Borgne, The galaxy population hosting gamma-ray bursts, Astrophys. J. 691 (2009) 182–211.
[45] S.E. Woosley, A. Heger, The progenitor stars of gamma-ray bursts, Astrophys. J. 637 (2006) 914–921.
[46] C.L. Fryer, S.E. Woosley, D.H. Hartmann, Formation rates of black hole accretion disk gamma-ray bursts, Astrophys. J. 526 (1999) 152–177.
[47] S.-C. Yoon, N. Langer, Evolution of rapidly rotating metal-poor massive stars towards gamma-ray bursts, Astron. Astrophys. 443 (2005) 643–648.
[48] M. Vietri, L. Stella, A gamma-ray burst model with small baryon contamination, Astrophys. J. 507 (1998) L45–L48.
[49] A.M. Soderberg, et al., Relativistic ejecta from X-ray flash XRF 060218 and the rate of cosmic explosions, Nature 442 (2006) 1014–1017.
[50] P.A. Mazzali, et al., A neutron-star-driven X-ray flash associated with supernova SN 2006aj, Nature 442 (2006) 1018–1020.

[51] E. Liang, et al., Low-luminosity gamma-ray bursts as a unique population: Luminosity function, local rate, and beaming factor, Astrophys. J. 662 (2007) 1111–1118.
[52] S.T. Holland, et al., GRB 090417B and its host galaxy: A step toward an understanding of optically dark gamma-ray bursts, Astrophys. J. 717 (2010) 223–234.
[53] C. Wolf, P. Podsiadlowski, The metallicity dependence of the long-duration gamma-ray burst rate from host galaxy luminosities, Month. Not. Roy. Astron. Soc. 375 (2007) 1049–1058.
[54] L.-X. Li, Star formation history up to $z = 7.4$: implications for gamma-ray bursts and cosmic metallicity evolution, Month. Not. Roy. Astron. Soc. 388 (2008) 1487–1500.
[55] Y. Niino, et al., Luminosity distribution of gamma-ray burst host galaxies at redshift $z = 1$ in cosmological smoothed particle hydrodynamic simulations: Implications for the metallicity dependence of GRBs, Astrophys. J. 726 (2011) 88.
[56] J.S. Bloom, et al., Closing in on a short-hard burst progenitor: Constraints from early-time optical imaging and spectroscopy of a possible host galaxy of GRB 050509b, Astrophys. J. 638 (2006) 354–368.
[57] W. Fong, E. Berger, D.B. Fox, Hubble space telescope observations of short gamma-ray burst host galaxies: Morphologies, offsets, and local environments, Astrophys. J. 708 (2010) 9–25.
[58] J. Hjorth, et al., The optical afterglow of the short γ-ray burst GRB 050709, Nature 437 (2005) 859–861.
[59] S. Rosswog, E. Ramirez-Ruiz, M.B. Davies, High-resolution calculations of merging neutron stars – III. Gamma-ray bursts, Month. Not. Roy. Astron. Soc. 345 (2003) 1077–1090.
[60] M.A. Aloy, H.-T. Janka, E. Müller, Relativistic outflows from remnants of compact object mergers and their viability for short gamma-ray bursts, Astron. Astrophys. 436 (2005) 273–311.
[61] L. Rezzolla, et al., The missing link: merging neutron stars naturally produce jet-like structures and can power short gamma-ray bursts, arXiv:1101.4298.
[62] B. Paczýnski, Cosmological gamma-ray bursts, Acta Astron. 41 (1991) 257–267.
[63] J.H. Taylor, J.M. Weisberg, Further experimental tests of relativistic gravity using the binary pulsar PSR 1913 + 16, Astrophys. J. 345 (1989) 434–450.
[64] M. Kramer, I.H. Stairs, The double pulsar, Annu. Rev. Astron. Astrophys. 46 (2008) 541–572.
[65] E. Nakar, Short-hard gamma-ray bursts, Phys. Rep. 442 (2007) 166–236.
[66] W.H. Lee, E. Ramirez-Ruiz, The progenitors of short gamma-ray bursts, New J. Phys. 9 (2007) 17.
[67] E. Berger, et al., A new population of high-redshift short-duration gamma-ray bursts, Astrophys. J. 664 (2007) 1000–1010.
[68] A. de Ugarte Postigo, et al., GRB 060121: Implications of a short-/intermediate-duration γ-ray burst at high redshift, Astrophys. J. 648 (2006) L83–L87.
[69] F.J. Virgili, B. Zhang, P. O'Brien, E. Troja, Are all short-hard gamma-ray bursts produced from mergers of compact stellar objects?, Astrophys. J. 727 (2011) 109.
[70] E. Nakar, A. Gal-Yam, D.B. Fox, The local rate and the progenitor lifetimes of short-hard gamma-ray bursts: Synthesis and predictions for the laser interferometer gravitational-wave observatory, Astrophys. J. 650 (2006) 281–290.
[71] D. Guetta, T. Piran, The BATSE-Swift luminosity and redshift distributions of short-duration GRBs, Astron. Astrophys. 453 (2006) 823–828.
[72] W.H. Lee, E. Ramirez-Ruiz, G. van de Ven, Short gamma-ray bursts from dynamically assembled compact binaries in globular clusters: Pathways, rates, hydrodynamics, and cosmological setting, Astrophys. J. 720 (2010) 953–975.
[73] S. Rosswog, invited talk at "Prompt GRB 2011", Raleigh.
[74] C. Cutler, K.S. Thorne, An overview of gravitational-wave sources, arXiv:gr-qc/0204090, 2002.
[75] C.D. Dermer, A. Atoyan, Collapse of neutron stars to black holes in binary systems: A model for short gamma-ray bursts, Astrophys. J. 643 (2006) L13–L16.
[76] D.M. Palmer, et al., A giant γ-ray flare from the magnetar SGR 1806-20, Nature 434 (2005) 1107–1109.
[77] K. Hurley, et al., An exceptionally bright flare from SGR 1806-20 and the origins of short-duration γ-ray bursts, Nature 434 (2005) 1098–1103.
[78] N.R. Tanvir, et al., An origin in the local universe for some short γ-ray bursts, Nature 438 (2005) 991–993.
[79] E. Nakar, et al., The distances of short-hard gamma-ray bursts and the soft gamma-ray repeater connection, Astrophys. J. 640 (2006) 849–853.
[80] G.J. Fishman, C.A. Meegan, Gamma-ray bursts, Annu. Rev. Astron. Astrophys. 33 (1995) 415–458.
[81] B. Zhang, P. Mészáros, Gamma-ray bursts progress, problems & prospects, Internat. J. Modern Phys. A 19 (2004) 2385–2472.
[82] T. Piran, Gamma-ray bursts and the fireball model, Phys. Rep. 314 (1999) 575–667.
[83] Y. Lithwick, R. Sari, Lower limits on Lorentz factors in gamma-ray bursts, Astrophys. J. 555 (2001) 540–545.
[84] E.-W. Liang, et al., Constraining GRB initial Lorentz factor with the afterglow onset feature and discovery of a tight Γ_0–E_{iso} correlation, Astrophys. J. 725 (2010) 2209–2224.
[85] A.A. Abdo, et al., Fermi observations of high-energy gamma-ray emission from GRB 080916C, Science 323 (2009) 1688–1693.
[86] A.A. Abdo, et al., A limit on the variation of the speed of light arising from quantum gravity effects, Nature 462 (2009) 331–334.
[87] A.A. Abdo, et al., Fermi observations of GRB 090902B: A distinct spectral component in the prompt and delayed emission, Astrophys. J. 706 (2009) L138–L144.
[88] D.A. Frail, et al., Beaming in gamma-ray bursts: Evidence for a standard energy reservoir, Astrophys. J. 562 (2001) L55–L58.
[89] J.S. Bloom, D.A. Frail, S.R. Kulkarni, Gamma-ray burst energetics and the gamma-ray burst Hubble diagram: Promises and limitations, Astrophys. J. 594 (2003) 674–683.
[90] E.-W. Liang, et al., A comprehensive analysis of Swift XRT data. III. Jet break candidates in X-ray and optical afterglow light curves, Astrophys. J. 675 (2008) 528–552.
[91] J.L. Racusin, et al., Jet breaks and energetics of Swift GRB X-ray afterglows, Astrophys. J. 698 (2009) 43–74.
[92] A.M. Beloborodov, B.E. Stern, R. Svensson, Self-similar temporal behavior of gamma-ray bursts, Astrophys. J. 508 (1998) L25–L27.
[93] J.P. Norris, Implications of the lag-luminosity relationship for unified gamma-ray burst paradigms, Astrophys. J. 579 (2002) 386–403.
[94] A.I. MacFadyen, S.E. Woosley, Collapsars: Gamma-ray bursts and explosions in "failed supernovae", Astrophys. J. 524 (1999) 262–289.
[95] D. Proga, et al., Axisymmetric magnetohydrodynamic simulations of the collapsar model for gamma-ray bursts, Astrophys. J. 599 (2003) L5–L8.
[96] W. Zhang, S.E. Woosley, A.I. MacFadyen, Relativistic jets in collapsars, Astrophys. J. 586 (2003) 356–371.
[97] B.J. Morsony, D. Lazzati, M.C. Begelman, The origin and propagation of variability in the outflows of long-duration gamma-ray bursts, Astrophys. J. 723 (2010) 267–276.
[98] R.D. Blandford, R.L. Znajek, Electromagnetic extraction of energy from Kerr black holes, Month. Not. Roy. Astron. Soc. 179 (1977) 433–456.
[99] P. Mészáros, M.J. Rees, Poynting jets from black holes and cosmological gamma-ray bursts, Astrophys. J. 482 (1997) L29–L32.
[100] H.K. Lee, R.A.M.J. Wijers, G.E. Brown, The Blandford–Znajek process as a central engine for a gamma-ray burst, Phys. Rep. 325 (2000) 83–114.
[101] L.-X. Li, Extracting energy from a black hole through its disk, Astrophys. J. 533 (2000) L115–L118.
[102] J.C. McKinney, Total and jet Blandford–Znajek power in the presence of an accretion disk, Astrophys. J. 630 (2005) L5–L8.
[103] D. Proga, M.C. Begelman, Accretion of low angular momentum material onto black holes: Two-dimensional magnetohydrodynamic case, Astrophys. J. 592 (2003) 767–781.
[104] W.H. Lei, et al., Magnetically torqued neutrino-dominated accretion flows for gamma-ray bursts, Astrophys. J. 700 (2009) 1970–1976.

[105] V.V. Usov, Millisecond pulsars with extremely strong magnetic fields as a cosmological source of gamma-ray bursts, Nature 357 (1992) 472–474.
[106] D. Zhang, Z.G. Dai, Hyperaccreting neutron star disks and neutrino annihilation, Astrophys. J. 703 (2009) 461–478.
[107] H.-T. Janka, E. Mueller, The first second of a type II supernova: Convection, accretion, and shock propagation, Astrophys. J. 448 (1995) L109–L113.
[108] Y.-Z. Qian, S.E. Woosley, Nucleosynthesis in neutrino-driven winds. I. The physical condition, Astrophys. J. 471 (1996) 331–351.
[109] T.A. Thompson, P. Chang, E. Quataert, Magnetar spin-down, hyperenergetic supernovae, and gamma-ray bursts, Astrophys. J. 611 (2004) 380–393.
[110] B.D. Metzger, T.A. Thompson, E. Quataert, Proto-neutron star winds with magnetic fields and rotation, Astrophys. J. 659 (2007) 561–579.
[111] B.D. Metzger, et al., The proto-magnetar model for gamma-ray bursts, Month. Not. Roy. Astron. Soc., submitted for publication, arXiv:1012.0001.
[112] J.C. Wheeler, et al., Asymmetric supernovae, pulsars, magnetars, and gamma-ray bursts, Astrophys. J. 537 (2000) 810–823.
[113] M. Lyutikov, R. Blandford, Gamma ray bursts as electromagnetic outflows, arXiv:astro-ph/0312347, 2003.
[114] E. Witten, Cosmic separation of phases, Phys. Rev. D 30 (1984) 272–285.
[115] C. Alcock, E. Farhi, A. Olinto, Strange stars, Astrophys. J. 310 (1986) 261–272.
[116] K.S. Cheng, Z.G. Dai, Conversion of neutron stars to strange stars as a possible origin of γ-ray bursts, Phys. Rev. Lett. 77 (1996) 1210–1213.
[117] Z.G. Dai, T. Lu, γ-Ray bursts and afterglows from rotating strange stars and neutron stars, Phys. Rev. Lett. 81 (1998) 4301–4304.
[118] R. Ouyed, R. Rapp, C. Vogt, Fireballs from quark stars in the color-flavor locked phase: Application to gamma-ray bursts, Astrophys. J. 632 (2005) 1001–1007.
[119] B. Paczyński, P. Haensel, Gamma-ray bursts from quark stars, Month. Not. Roy. Astron. Soc. 362 (2005) L4–L7.
[120] R. Xu, E. Liang, X-ray flares of γ-ray bursts: Quakes of solid quark stars?, Sci. China G: Phys. Astron. 52 (2009) 315–320.
[121] K. Iwamoto, et al., A hypernova model for the supernova associated with the γ-ray burst of 25 April 1998, Nature 395 (1998) 672–674.
[122] P.A. Mazzali, et al., The type Ic hypernova SN 2003dh/GRB 030329, Astrophys. J. 599 (2003) L95–L98.
[123] Z.G. Dai, T. Lu, Gamma-ray burst afterglows and evolution of postburst fireballs with energy injection from strongly magnetic millisecond pulsars, Astron. Astrophys. 333 (1998) L87–L90.
[124] B. Zhang, P. Mészáros, Gamma-ray burst afterglow with continuous energy injection: Signature of a highly magnetized millisecond pulsar, Astrophys. J. 552 (2001) L35–L38.
[125] B. Zhang, et al., Physical processes shaping gamma-ray burst X-ray afterglow light curves: Theoretical implications from the Swift X-ray telescope observations, Astrophys. J. 642 (2006) 354–370.
[126] J.A. Nousek, et al., Evidence for a canonical gamma-ray burst afterglow light curve in the Swift XRT data, Astrophys. J. 642 (2006) 389–400.
[127] P.T. O'Brien, et al., The early X-ray emission from GRBs, Astrophys. J. 647 (2006) 1213–1237.
[128] E. Troja, et al., Swift observations of GRB 070110: An extraordinary X-ray afterglow powered by the central engine, Astrophys. J. 665 (2007) 599–607.
[129] E.-W. Liang, B.-B. Zhang, B. Zhang, A comprehensive analysis of Swift XRT data. II. Diverse physical origins of the shallow decay segment, Astrophys. J. 670 (2007) 565–583.
[130] N. Lyons, et al., Can X-ray emission powered by a spinning-down magnetar explain some gamma-ray burst light-curve features?, Month. Not. Roy. Astron. Soc. 402 (2010) 705–712.
[131] J. Novak, Numerical simulations of GRB engines, C. R. Physique 12 (2011) 246–254 (this issue).
[132] E.V. Derishev, V.V. Kocharovsky, V.V. Kocharovsky, The neutron component in fireballs of gamma-ray bursts: Dynamics and observable imprints, Astrophys. J. 521 (1999) 640–649.
[133] A.M. Beloborodov, Nuclear composition of gamma-ray burst fireballs, Astrophys. J. 588 (2003) 931–944.
[134] A.M. Beloborodov, Neutron-fed afterglows of gamma-ray bursts, Astrophys. J. 585 (2003) L19–L22.
[135] Y.Z. Fan, B. Zhang, D.M. Wei, Early optical afterglow light curves of neutron-fed gamma-ray bursts, Astrophys. J. 628 (2005) 298–314.
[136] J. Goodman, Are gamma-ray bursts optically thick?, Astrophys. J. 308 (1986) L47–L50.
[137] A. Shemi, T. Piran, The appearance of cosmic fireballs, Astrophys. J. 365 (1990) L55–L58.
[138] M.J. Rees, P. Mészáros, Relativistic fireballs – Energy conversion and time-scales, Month. Not. Roy. Astron. Soc. 258 (1992) 41P–43P.
[139] P. Mészáros, M.J. Rees, Relativistic fireballs and their impact on external matter – Models for cosmological gamma-ray bursts, Astrophys. J. 405 (1993) 278–284.
[140] M.J. Rees, P. Mészáros, Unsteady outflow models for cosmological gamma-ray bursts, Astrophys. J. 430 (1994) L93–L96.
[141] G. Drenkhahn, H.C. Spruit, Efficient acceleration and radiation in Poynting flux powered GRB outflows, Astron. Astrophys. 391 (2002) 1141–1153.
[142] N. Vlahakis, A. Königl, Relativistic magnetohydrodynamics with application to gamma-ray burst outflows. I. Theory and semianalytic trans-Alfvénic solutions, Astrophys. J. 596 (2003) 1080–1103.
[143] S.S. Komissarov, et al., Magnetic acceleration of ultrarelativistic jets in gamma-ray burst sources, Month. Not. Roy. Astron. Soc. 394 (2009) 1182–1212.
[144] A. Tchekhovskoy, J.C. McKinney, R. Narayan, Efficiency of magnetic to kinetic energy conversion in a monopole magnetosphere, Astrophys. J. 699 (2009) 1789–1808.
[145] B. Zhang, H. Yan, The internal-collision-induced magnetic reconnection and turbulence (ICMART) model of gamma-ray bursts, Astrophys. J. 726 (2011) 90.
[146] E. Waxman, Astronomy: New direction for γ-rays, Nature 423 (2003) 388–389.
[147] M. Lyutikov, V.I. Pariev, R.D. Blandford, Polarization of prompt gamma-ray burst emission: Evidence for electromagnetically dominated outflow, Astrophys. J. 597 (2003) 998–1009.
[148] J. Granot, The most probable cause for the high gamma-ray polarization in GRB 021206, Astrophys. J. 596 (2003) L17–L21.
[149] K. Toma, et al., Statistical properties of gamma-ray burst polarization, Astrophys. J. 698 (2009) 1042–1053.
[150] W. Coburn, S.E. Boggs, Polarization of the prompt γ-ray emission from the γ-ray burst of 6 December 2002, Nature 423 (2003) 415–417.
[151] D.R. Willis, et al., Evidence of polarisation in the prompt gamma-ray emission from GRB 930131 and GRB 960924, Astron. Astrophys. 439 (2005) 245–253.
[152] R.E. Rutledge, D.B. Fox, Re-analysis of polarization in the γ-ray flux of GRB 021206, Month. Not. Roy. Astron. Soc. 350 (2004) 1288–1300.
[153] B. Zhang, A. Pe'er, Evidence of an initially magnetically dominated outflow in GRB 080916C, Astrophys. J. 700 (2009) L65–L68.
[154] Y.-Z. Fan, The spectrum of γ-ray burst: a clue, Month. Not. Roy. Astron. Soc. 403 (2010) 483–490.
[155] B.-B. Zhang, et al., A comprehensive analysis of Fermi gamma-ray burst data. I. Spectral components and their possible physical origins of LAT/GBM GRBs, Astrophys. J. 730 (2011) 141, doi:10.1088/0004-637X/730/2/141, arXiv:1009.3338.
[156] A.M. Beloborodov, Collisional mechanism for gamma-ray burst emission, Month. Not. Roy. Astron. Soc. 407 (2010) 1033–1047.
[157] D. Lazzati, M.C. Begelman, Non-thermal emission from the photospheres of gamma-ray burst outflows. I: High frequency tails, Astrophys. J. 725 (2010) 1137–1145.
[158] M. Ackermann, et al., Fermi observations of GRB 090510: A short-hard gamma-ray burst with an additional, hard power-law component from 10 keV to GeV energies, Astrophys. J. 716 (2010) 1178–1190.
[159] F. Ryde, et al., Identification and properties of the photospheric emission in GRB090902B, Astrophys. J. 709 (2010) L172–L177.
[160] A. Pe'er, et al., The connection between thermal and non-thermal emission in gamma-ray bursts: General considerations and GRB090902B as a case study, Astrophys. J. (2010), submitted for publication, arXiv:1007.2228.
[161] Y.Z. Fan, D.M. Wei, C.F. Wang, The very early afterglow powered by ultra-relativistic mildly magnetized outflows, Astron. Astrophys. 424 (2004) 477–484.

[162] B. Zhang, S. Kobayashi, Gamma-ray burst early afterglows reverse shock emission from an arbitrarily magnetized ejecta, Astrophys. J. 628 (2005) 315–334.
[163] P. Mimica, D. Giannios, M.A. Aloy, Deceleration of arbitrarily magnetized GRB ejecta: the complete evolution, Astron. Astrophys. 494 (2009) 879–890.
[164] Y. Mizuno, et al., Magnetohydrodynamic effects in propagating relativistic jets: Reverse shock and magnetic acceleration, Astrophys. J. 690 (2009) L47–L51.
[165] Y.-Z. Fan, et al., Optical flash of GRB 990123: Constraints on the physical parameters of the reverse shock, Chinese J. Astron. Astrophys. 2 (2002) 449–453.
[166] B. Zhang, S. Kobayashi, P. Mészáros, Gamma-ray burst early optical afterglows: Implications for the initial Lorentz factor and the central engine, Astrophys. J. 595 (2003) 950–954.
[167] P. Kumar, A. Panaitescu, A unified treatment of the gamma-ray burst 021211 and its afterglow, Month. Not. Roy. Astron. Soc. 346 (2003) 905–914.
[168] A. Gomboc, et al., Multiwavelength analysis of the intriguing GRB 061126: The reverse shock scenario and magnetization, Astrophys. J. 687 (2008) 443–455.
[169] I.A. Steele, et al., Ten per cent polarized optical emission from GRB 090102, Nature 462 (2009) 767–769.
[170] J.C. McKinney, D.A. Uzdensky, A reconnection switch to trigger gamma-ray burst jet dissipation, Month. Not. Roy. Astron. Soc., submitted for publication, arXiv:1011.1904.
[171] G. Tagliaferri, et al., An unexpectedly rapid decline in the X-ray afterglow emission of long γ-ray bursts, Nature 436 (2005) 985–988.
[172] S.D. Barthelmy, et al., Discovery of an afterglow extension of the prompt phase of two gamma-ray bursts observed by Swift, Astrophys. J. 635 (2005) L133–L136.
[173] B.-B. Zhang, E.-W. Liang, B. Zhang, A comprehensive analysis of Swift XRT data. I. Apparent spectral evolution of gamma-ray burst X-ray tails, Astrophys. J. 666 (2007) 1002–1011.
[174] P. Kumar, A. Panaitescu, Afterglow emission from naked gamma-ray bursts, Astrophys. J. 541 (2000) L51–L54.
[175] E.W. Liang, et al., Testing the curvature effect and internal origin of gamma-ray burst prompt emissions and X-ray flares with Swift data, Astrophys. J. 646 (2006) 351–357.
[176] B.-B. Zhang, et al., Curvature effect of a non-power spectrum and spectral evolution of GRB X-ray tails, Astrophys. J. 690 (2009) L10–L13.
[177] M. Lyutikov, Did Swift measure gamma-ray burst prompt emission radii?, Month. Not. Roy. Astron. Soc. 369 (2006) L5–L8.
[178] P. Kumar, et al., A unified picture for gamma-ray burst prompt and X-ray afterglow emissions, Month. Not. Roy. Astron. Soc. 367 (2006) L52–L56.
[179] W.T. Vestrand, et al., A link between prompt optical and prompt γ-ray emission in γ-ray bursts, Nature 435 (2005) 178–180.
[180] J.L. Racusin, et al., Broadband observations of the naked-eye γ-ray burst GRB080319B, Nature 455 (2008) 183–188.
[181] P. Kumar, A. Panaitescu, What did we learn from gamma-ray burst 080319B?, Month. Not. Roy. Astron. Soc. 391 (2008) L19–L23.
[182] R.-F. Shen, B. Zhang, Prompt optical emission and synchrotron self-absorption constraints on emission site of GRBs, Month. Not. Roy. Astron. Soc. 398 (2009) 1936–1950.
[183] N. Gupta, B. Zhang, Diagnosing the site of gamma-ray burst prompt emission with spectral cut-off energy, Month. Not. Roy. Astron. Soc. 384 (2008) L11–L15.
[184] P. Kumar, et al., The nature of the outflow in gamma-ray bursts, Month. Not. Roy. Astron. Soc. 376 (2007) L57–L61.
[185] P. Kumar, E. McMahon, A general scheme for modelling γ-ray burst prompt emission, Month. Not. Roy. Astron. Soc. 384 (2008) 33–63.
[186] Y.-Z. Fan, B. Zhang, D.-M. Wei, Naked-eye optical flash from gamma-ray burst 080319B: Tracing the decaying neutrons in the outflow, Phys. Rev. D 79 (2) (2009) 021301.
[187] Y.-C. Zou, T. Piran, R. Sari, Clues from the prompt emission of GRB 080319B, Astrophys. J. 692 (2009) L92–L95.
[188] L. Resmi, B. Zhang, Gamma ray burst prompt emission variability in synchrotron and synchrotron self-Compton lightcurves, Month. Not. Roy. Astron. Soc. (2010), submitted for publication.
[189] E. Waxman, Cosmological gamma-ray bursts and the highest energy cosmic rays, Phys. Rev. Lett. 75 (1995) 386–389.
[190] M. Vietri, The acceleration of ultra-high-energy cosmic rays in gamma-ray bursts, Astrophys. J. 453 (1995) 883–889.
[191] E. Waxman, J. Bahcall, High energy neutrinos from cosmological gamma-ray burst fireballs, Phys. Rev. Lett. 78 (1997) 2292–2295.
[192] P. Mészáros, E. Waxman, TeV neutrinos from successful and choked gamma-ray bursts, Phys. Rev. Lett. 87 (17) (2001) 171102.
[193] S. Razzaque, P. Mészáros, E. Waxman, Neutrino signatures of the supernova: Gamma ray burst relationship, Phys. Rev. D 69 (2) (2004) 023001.
[194] B. Paczýnski, G. Xu, Neutrino bursts from gamma-ray bursts, Astrophys. J. 427 (1994) 708–713.
[195] P. Mészáros, P. Laguna, M.J. Rees, Gas dynamics of relativistically expanding gamma-ray burst sources – Kinematics, energetics, magnetic fields, and efficiency, Astrophys. J. 415 (1993) 181–190.
[196] P. Mészáros, M.J. Rees, Optical and long-wavelength afterglow from gamma-ray bursts, Astrophys. J. 476 (1997) 232.
[197] R. Sari, T. Piran, GRB 990123: The optical flash and the fireball model, Astrophys. J. 517 (1999) L109–L112.
[198] S. Kobayashi, Light curves of gamma-ray burst optical flashes, Astrophys. J. 545 (2000) 807–812.
[199] R. Sari, T. Piran, Hydrodynamic timescales and temporal structure of gamma-ray bursts, Astrophys. J. 455 (1995) L143–L146.
[200] R.D. Blandford, C.F. McKee, Fluid dynamics of relativistic blast waves, Phys. Fluids 19 (1976) 1130–1138.
[201] M.J. Rees, P. Mészáros, Refreshed shocks and afterglow longevity in gamma-ray bursts, Astrophys. J. 496 (1998) L1–L4.
[202] K.-I. Nishikawa, et al., Particle acceleration and magnetic field generation in electron–positron relativistic shocks, Astrophys. J. 622 (2005) 927–937.
[203] A. Spitkovsky, Particle acceleration in relativistic collisionless shocks: Fermi process at last? Astrophys. J. 682 (2008) L5–L8.
[204] K.-I. Nishikawa, et al., Weibel instability and associated strong fields in a fully three-dimensional simulation of a relativistic shock, Astrophys. J. 698 (2009) L10–L13.
[205] C.F. Kennel, F.V. Coroniti, Confinement of the Crab pulsar's wind by its supernova remnant, Astrophys. J. 283 (1984) 694–709.
[206] L. Sironi, A. Spitkovsky, Particle acceleration in relativistic magnetized collisionless pair shocks: Dependence of shock acceleration on magnetic obliquity, Astrophys. J. 698 (2009) 1523–1549.
[207] P.A. Sweet, The neutral point theory of solar flares, in: B. Lehnert (Ed.), Electromagnetic Phenomena in Cosmical Physics, in: IAU Symposium, vol. 6, 1958, pp. 123–134.
[208] E.N. Parker, Sweet's mechanism for merging magnetic fields in conducting fluids, J. Geophys. Res. 62 (1957) 509–520.
[209] C. Thompson, A model of gamma-ray bursts, Month. Not. Roy. Astron. Soc. 270 (1994) 480.
[210] M.J. Rees, P. Mészáros, Dissipative photosphere models of gamma-ray bursts and X-ray flashes, Astrophys. J. 628 (2005) 847–852.
[211] C. Thompson, P. Mészáros, M.J. Rees, Thermalization in relativistic outflows and the correlation between spectral hardness and apparent luminosity in gamma-ray bursts, Astrophys. J. 666 (2007) 1012–1023.
[212] A. Lazarian, E.T. Vishniac, Reconnection in a weakly stochastic field, Astrophys. J. 517 (1999) 700–718.
[213] E. Liang, K. Noguchi, Radiation from comoving Poynting flux acceleration, Astrophys. J. 705 (2009) 1473–1480.
[214] M.V. Smolsky, V.V. Usov, Relativistic beam–magnetic barrier collision and nonthermal radiation of cosmological γ-ray bursters, Astrophys. J. 461 (1996) 858–871.
[215] J.S.T. Ng, R.J. Noble, Inductive and electrostatic acceleration in relativistic jet–plasma interactions, Phys. Rev. Lett. 96 (11) (2006) 115006.
[216] M. Lemoine, G. Pelletier, Shock acceleration in gamma-ray bursts, C. R. Physique 12 (2011) 234–245 (this issue).

[217] D. Band, et al., BATSE observations of gamma-ray burst spectra. I – Spectral diversity, Astrophys. J. 413 (1993) 281–292.
[218] P. Mészáros, M.J. Rees, H. Papathanassiou, Spectral properties of blast-wave models of gamma-ray burst sources, Astrophys. J. 432 (1994) 181–193.
[219] M. Tavani, A shock emission model for gamma-ray bursts. II. Spectral properties, Astrophys. J. 466 (1996) 768–778.
[220] M.V. Medvedev, A. Loeb, Generation of magnetic fields in the relativistic shock of gamma-ray burst sources, Astrophys. J. 526 (1999) 697–706.
[221] G. Ghisellini, A. Celotti, D. Lazzati, Constraints on the emission mechanisms of gamma-ray bursts, Month. Not. Roy. Astron. Soc. 313 (2000) L1–L5.
[222] A. Pe'er, B. Zhang, Synchrotron emission in small-scale magnetic fields as a possible explanation for prompt emission spectra of gamma-ray bursts, Astrophys. J. 653 (2006) 454–461.
[223] K. Asano, T. Terasawa, Slow heating model of gamma-ray burst: Photon spectrum and delayed emission, Astrophys. J. 705 (2009) 1714–1720.
[224] F. Daigne, Z. Bosnjak, G. Dubus, Reconciling observed GRB prompt spectra with synchrotron radiation?, Astron. Astrophys. 526 (2011) 110.
[225] R.D. Preece, et al., The synchrotron shock model confronts a "line of death" in the BATSE gamma-ray burst data, Astrophys. J. 506 (1998) L23–L26.
[226] P. Mészáros, M.J. Rees, Steep slopes and preferred breaks in gamma-ray burst spectra: The role of photospheres and comptonization, Astrophys. J. 530 (2000) 292–298.
[227] N.M. Lloyd, V. Petrosian, Synchrotron radiation as the source of gamma-ray burst spectra, Astrophys. J. 543 (2000) 722–732.
[228] M.V. Medvedev, Theory of "jitter" radiation from small-scale random magnetic fields and prompt emission from gamma-ray burst shocks, Astrophys. J. 540 (2000) 704–714.
[229] F. Daigne, R. Mochkovitch, Gamma-ray bursts from internal shocks in a relativistic wind: temporal and spectral properties, Month. Not. Roy. Astron. Soc. 296 (1998) 275–286.
[230] A.M. Bykov, P. Meszaros, Electron acceleration and efficiency in nonthermal gamma-ray sources, Astrophys. J. 461 (1996) L37–L40.
[231] M.V. Medvedev, Electron acceleration in relativistic gamma-ray burst shocks, Astrophys. J. 651 (2006) L9–L11.
[232] L. Sironi, A. Spitkovsky, Synthetic spectra from particle-in-cell simulations of relativistic collisionless shocks, Astrophys. J. 707 (2009) L92–L96.
[233] S. Zenitani, M. Hesse, The role of the Weibel instability at the reconnection jet front in relativistic pair plasma reconnection, Phys. Plasma 15 (2008) 022101.
[234] A. Panaitescu, P. Mészáros, Gamma-ray bursts from upscattered self-absorbed synchrotron emission, Astrophys. J. 544 (2000) L17–L21.
[235] Z. Bosnjak, D. Daigne, G. Dubus, Prompt high-energy emission from gamma-ray bursts in the internal shock model, Astron. Astrophys. 498 (2009) 677–703.
[236] P. Kumar, R. Narayan, GRB 080319B: evidence for relativistic turbulence, not internal shocks, Month. Not. Roy. Astron. Soc. 395 (2009) 472–489.
[237] E.V. Derishev, V.V. Kocharovsky, V.V. Kocharovsky, Physical parameters and emission mechanism in gamma-ray bursts, Astron. Astrophys. 372 (2001) 1071–1077.
[238] T. Piran, R. Sari, Y.-C. Zou, Observational limits on inverse Compton processes in gamma-ray bursts, Month. Not. Roy. Astron. Soc. 393 (2009) 1107–1113.
[239] G. Beskin, et al., Fast optical variability of a naked-eye burst – Manifestation of the periodic activity of an internal engine, Astrophys. J. 719 (2010) L10–L14.
[240] A. Pe'er, P. Mészáros, M.J. Rees, The observable effects of a photospheric component on GRB and XRF prompt emission spectrum, Astrophys. J. 642 (2006) 995–1003.
[241] C. Thompson, Deceleration of a relativistic, photon-rich shell: End of preacceleration, damping of magnetohydrodynamic turbulence, and the emission mechanism of gamma-ray bursts, Astrophys. J. 651 (2006) 333–365.
[242] D. Giannios, Prompt GRB emission from gradual energy dissipation, Astron. Astrophys. 480 (2008) 305–312.
[243] A. Pe'er, F. Ryde, A theory of multicolor black body emission from relativistically expanding plasmas, Astrophys. J. (2010), submitted for publication, arXiv:1008.4590.
[244] D. Lazzati, et al., Compton-dragged gamma-ray bursts associated with supernovae, Astrophys. J. 529 (2000) L17–L20.
[245] A. Dar, A. de Rújula, Towards a complete theory of gamma-ray bursts, Phys. Rep. 405 (2004) 203–278.
[246] X.-Y. Wang, et al., Nonthermal gamma-ray/X-ray flashes from shock breakout in gamma-ray burst-associated supernovae, Astrophys. J. 664 (2007) 1026–1032.
[247] N. Gupta, B. Zhang, Prompt emission of high-energy photons from gamma ray bursts, Month. Not. Roy. Astron. Soc. 380 (2007) 78–92.
[248] K. Asano, S. Inoue, P. Mészáros, Prompt high-energy emission from proton-dominated gamma-ray bursts, Astrophys. J. 699 (2009) 953–957.
[249] S. Razzaque, C.D. Dermer, J.D. Fink, Synchrotron radiation from ultra-high energy protons and the Fermi observations of GRB 080916C, Open Astron. J. 1 (2010) 150–155.
[250] N.J. Shaviv, A. Dar, Gamma-ray bursts from minijets, Astrophys. J. 447 (1995) 863–873.
[251] D. Lazzati, et al., Compton drag as a mechanism for very high linear polarization in gamma-ray bursts, Month. Not. Roy. Astron. Soc. 347 (2004) L1–L5.
[252] J.L. Atteia, M. Boer, Observing the prompt emission of GRBs, C. R. Physique 12 (2011) 255–266 (this issue).
[253] D.N. Burrows, et al., Bright X-ray flares in gamma-ray burst afterglows, Science 309 (2005) 1833–1835.
[254] G. Chincarini, et al., The first survey of X-ray flares from gamma-ray bursts observed by Swift: Temporal properties and morphology, Astrophys. J. 671 (2007) 1903–1920.
[255] A.D. Falcone, et al., The first survey of X-ray flares from gamma-ray bursts observed by Swift: Spectral properties and energetics, Astrophys. J. 671 (2007) 1921–1938.
[256] K. Ioka, S. Kobayashi, B. Zhang, Variabilities of gamma-ray burst afterglows: Long-acting engine, anisotropic jet, or many fluctuating regions?, Astrophys. J. 631 (2005) 429–434.
[257] Y.Z. Fan, D.M. Wei, Late internal-shock model for bright X-ray flares in gamma-ray burst afterglows and GRB 011121, Month. Not. Roy. Astron. Soc. 364 (2005) L42–L46.
[258] D. Lazzati, R. Perna, X-ray flares and the duration of engine activity in gamma-ray bursts, Month. Not. Roy. Astron. Soc. 375 (2007) L46–L50.
[259] A. Maxham, B. Zhang, Modeling gamma-ray burst X-ray flares within the internal shock model, Astrophys. J. 707 (2009) 1623–1633.
[260] A.M. Beloborodov, et al., Is GRB afterglow emission intrinsically anisotropic?, Month. Not. Roy. Astron. Soc. 410 (2011) 2422–2427, doi:10.1111/j.1365-2966.2010.17616.x, arXiv:1003.1265.
[261] R. Sari, P. Mészáros, Impulsive and varying injection in gamma-ray burst afterglows, Astrophys. J. 535 (2000) L33–L37.
[262] G. Ghisellini, et al., "Late prompt" emission in gamma-ray bursts?, Astrophys. J. 658 (2007) L75–L78.
[263] P. Kumar, R. Narayan, J.L. Johnson, Mass fall-back and accretion in the central engine of gamma-ray bursts, Month. Not. Roy. Astron. Soc. 388 (2008) 1729–1742.
[264] J.K. Cannizzo, N. Gehrels, A new paradigm for gamma-ray bursts: Long-term accretion rate modulation by an external accretion disk, Astrophys. J. 700 (2009) 1047–1058.
[265] C.C. Lindner, et al., Collapsar accretion and the gamma-ray burst X-ray light curve, Astrophys. J. 713 (2010) 800–815.
[266] A. Panaitescu, et al., Evidence for chromatic X-ray light-curve breaks in Swift gamma-ray burst afterglows and their theoretical implications, Month. Not. Roy. Astron. Soc. 369 (2006) 2059–2064.
[267] E.-W. Liang, et al., Temporal profiles and spectral lags of XRF 060218, Astrophys. J. 653 (2006) L81–L84.

[268] M. de Pasquale, et al., Jet breaks at the end of the slow decline phase of Swift GRB light curves, Month. Not. Roy. Astron. Soc. 392 (2009) 153–169.
[269] F. Genet, F. Daigne, R. Mochkovitch, Can the early X-ray afterglow of gamma-ray bursts be explained by a contribution from the reverse shock?, Month. Not. Roy. Astron. Soc. 381 (2007) 732–740.
[270] Z.L. Uhm, A.M. Beloborodov, On the mechanism of gamma-ray burst afterglows, Astrophys. J. 665 (2007) L93–L96.
[271] L. Shao, Z.G. Dai, A reverse-shock model for the early afterglow of GRB 050525A, Astrophys. J. 633 (2005) 1027–1030.
[272] R.-F. Shen, et al., The dust scattering model cannot explain the shallow X-ray decay in GRB afterglows, Month. Not. Roy. Astron. Soc. 393 (2009) 598–606.
[273] X.-F. Wu, B. Zhang, X-ray afterglow from photosphere of a long lasting engine-driven wind, Astrophys. J. (2011), submitted for publication.
[274] A. King, et al., Gamma-ray bursts: Restarting the engine, Astrophys. J. 630 (2005) L113–L115.
[275] R. Perna, P.J. Armitage, B. Zhang, Flares in long and short gamma-ray bursts: A common origin in a hyperaccreting accretion disk, Astrophys. J. 636 (2006) L29–L32.
[276] D. Proga, B. Zhang, The late time evolution of gamma-ray bursts: ending hyperaccretion and producing flares, Month. Not. Roy. Astron. Soc. 370 (2006) L61–L65.
[277] Z.G. Dai, et al., X-ray flares from postmerger millisecond pulsars, Science 311 (2006) 1127–1129.
[278] W.H. Lee, E. Ramirez-Ruiz, D. López-Cámara, Phase transitions and He-synthesis-driven winds in neutrino cooled accretion disks: Prospects for late flares in short gamma-ray bursts, Astrophys. J. 699 (2009) L93–L96.
[279] R. Popham, S.E. Woosley, C. Fryer, Hyperaccreting black holes and gamma-ray bursts, Astrophys. J. 518 (1999) 356–374.
[280] F. Yuan, et al., in preparation.
[281] Y.Z. Fan, B. Zhang, D. Proga, Linearly polarized X-ray flares following short gamma-ray bursts, Astrophys. J. 635 (2005) L129–L132.
[282] A.I. MacFadyen, S.E. Woosley, A. Heger, Supernovae, jets, and collapsars, Astrophys. J. 550 (2001) 410–425.
[283] S. Rosswog, Fallback accretion in the aftermath of a compact binary merger, Month. Not. Roy. Astron. Soc. 376 (2007) L48–L51.
[284] D. Lazzati, R. Perna, M.C. Begelman, X-ray flares, neutrino-cooled discs and the dynamics of late accretion in gamma-ray burst engines, Month. Not. Roy. Astron. Soc. 388 (2008) L15–L19.
[285] A. Corsi, P. Mészáros, Gamma-ray burst afterglow plateaus and gravitational waves: Multi-messenger signature of a millisecond magnetar?, Astrophys. J. 702 (2009) 1171–1178.
[286] R. Sari, T. Piran, R. Narayan, Spectra and light curves of gamma-ray burst afterglows, Astrophys. J. 497 (1998) L17.
[287] Z.G. Dai, T. Lu, Gamma-ray burst afterglows: effects of radiative corrections and non-uniformity of the surrounding medium, Month. Not. Roy. Astron. Soc. 298 (1998) 87–92.
[288] R.A. Chevalier, Z.-Y. Li, Wind interaction models for gamma-ray burst afterglows: The case for two types of progenitors, Astrophys. J. 536 (2000) 195–212.
[289] R.A.M.J. Wijers, T.J. Galama, Physical parameters of GRB 970508 and GRB 971214 from their afterglow synchrotron emission, Astrophys. J. 523 (1999) 177–186.
[290] A. Panaitescu, P. Kumar, Fundamental physical parameters of collimated gamma-ray burst afterglows, Astrophys. J. 560 (2001) L49–L53.
[291] A. Panaitescu, P. Kumar, Properties of relativistic jets in gamma-ray burst afterglows, Astrophys. J. 571 (2002) 779–789.
[292] S.A. Yost, et al., A study of the afterglows of four gamma-ray bursts: Constraining the explosion and fireball model, Astrophys. J. 597 (2003) 459–473.
[293] J.E. Rhoads, The dynamics and light curves of beamed gamma-ray burst afterglows, Astrophys. J. 525 (1999) 737–749.
[294] R. Sari, T. Piran, J.P. Halpern, Jets in gamma-ray bursts, Astrophys. J. 519 (1999) L17–L20.
[295] B. Zhang, P. Mészáros, Gamma-ray bursts with continuous energy injection and their afterglow signature, Astrophys. J. 566 (2002) 712–722.
[296] P. Mészáros, M.J. Rees, R.A.M.J. Wijers, Viewing angle and environment effects in gamma-ray bursts: Sources of afterglow diversity, Astrophys. J. 499 (1998) 301–308.
[297] B. Zhang, P. Mészáros, Gamma-ray burst beaming: A universal configuration with a standard energy reservoir?, Astrophys. J. 571 (2002) 876–879.
[298] E. Rossi, D. Lazzati, M.J. Rees, Afterglow light curves, viewing angle and the jet structure of γ-ray bursts, Month. Not. Roy. Astron. Soc. 332 (2002) 945–950.
[299] Y.F. Huang, Z.G. Dai, T. Lu, A generic dynamical model of gamma-ray burst remnants, Month. Not. Roy. Astron. Soc. 309 (1999) 513–516.
[300] Y.F. Huang, K.S. Cheng, Gamma-ray bursts: optical afterglows in the deep Newtonian phase, Month. Not. Roy. Astron. Soc. 341 (2003) 263–269.
[301] A. Panaitescu, et al., Analysis of the X-ray emission of nine Swift afterglows, Month. Not. Roy. Astron. Soc. 366 (2006) 1357–1366.
[302] D. Grupe, et al., Swift and XMM–Newton observations of the extraordinary gamma-ray burst 060729: More than 125 days of X-ray afterglow, Astrophys. J. 662 (2007) 443–458.
[303] V. Mangano, et al., Swift observations of GRB 060614: an anomalous burst with a well behaved afterglow, Astron. Astrophys. 470 (2007) 105–118.
[304] E. Berger, S.R. Kulkarni, D.A. Frail, A standard kinetic energy reservoir in gamma-ray burst afterglows, Astrophys. J. 590 (2003) 379–385.
[305] X. Dai, et al., Go long, go deep: Finding optical jet breaks for Swift-era GRBs with the LBT, Astrophys. J. 682 (2008) L77–L80.
[306] S. Kobayashi, B. Zhang, GRB 021004: Reverse shock emission, Astrophys. J. 582 (2003) L75–L78.
[307] C. Akerlof, et al., Observation of contemporaneous optical radiation from a γ-ray burst, Nature 398 (1999) 400–402.
[308] Z.P. Jin, Y.Z. Fan, GRB 060418 and 060607A: the medium surrounding the progenitor and the weak reverse shock emission, Month. Not. Roy. Astron. Soc. 378 (2007) 1043–1048.
[309] X.F. Wu, et al., Optical flashes and very early afterglows in wind environments, Month. Not. Roy. Astron. Soc. 342 (2003) 1131–1138.
[310] S. Kobayashi, B. Zhang, Early optical afterglows from wind-type gamma-ray bursts, Astrophys. J. 597 (2003) 455–458.
[311] S. Kobayashi, et al., Inverse Compton X-ray flare from gamma-ray burst reverse shock, Astrophys. J. 655 (2007) 391–395.
[312] X.Y. Wang, Z.G. Dai, T. Lu, Prompt high-energy gamma-ray emission from the synchrotron self-Compton process in the reverse shocks of gamma-ray bursts, Astrophys. J. 546 (2001) L33–L37.
[313] X.Y. Wang, Z.G. Dai, T. Lu, The inverse Compton emission spectra in the very early afterglows of gamma-ray bursts, Astrophys. J. 556 (2001) 1010–1016.
[314] O. Godet, R. Mochkovitch, Afterglows after Swift, C. R. Physique 12 (2011) 276–287 (this issue).
[315] K. Hurley, et al., Detection of a gamma-ray burst of very long duration and very high energy, Nature 372 (1994) 652–654.
[316] M.M. González, et al., A γ-ray burst with a high-energy spectral component inconsistent with the synchrotron shock model, Nature 424 (2003) 749–751.
[317] F. Piron, V. Connaughton, The Fermi view of gamma-ray bursts, C. R. Physique 12 (2011) 267–275 (this issue).
[318] M. Ackermann, et al., Detection of a spectral break in the extra hard component of GRB 090926A, Astrophys. J. 729 (2011) 114.
[319] G. Ghisellini, et al., GeV emission from gamma-ray bursts: a radiative fireball?, Month. Not. Roy. Astron. Soc. 403 (2010) 926–937.
[320] A. Maxham, B.-B. Zhang, B. Zhang, Is GeV emission from gamma-ray bursts of external shock origin?, Month. Not. Roy. Astron. Soc. (2011), in press, arXiv:1101.0144.
[321] K. Toma, X.-F. Wu, P. Mészáros, A photosphere-internal shock model of gamma-ray bursts: Implications for the Fermi/LAT results, Month. Not. Roy. Astron. Soc. (2010), submitted for publication, arXiv:1002.2634.
[322] P. Kumar, R. Barniol Duran, On the generation of high-energy photons detected by the Fermi satellite from gamma-ray bursts, Month. Not. Roy. Astron. Soc. 400 (2009) L75–L79.

[323] P. Kumar, R. Barniol Duran, External forward shock origin of high-energy emission for three gamma-ray bursts detected by Fermi, Month. Not. Roy. Astron. Soc. 409 (2010) 226–236.
[324] K. Toma, X.-F. Wu, P. Mészáros, An up-scattered cocoon emission model of gamma-ray burst high-energy lags, Astrophys. J. 707 (2009) 1404–1416.
[325] X.-Y. Wang, et al., Klein–Nishina effects on the high-energy afterglow emission of gamma-ray bursts, Astrophys. J. 712 (2010) 1232–1240.
[326] S.Y. Feng, Z.G. Dai, Multiband fitting to three long GRBs with Fermi/LAT data: Structured ejecta sweeping up a density-jump medium, Astrophys. J. (2010), submitted for publication, arXiv:1011.3103.
[327] H.-N. He, et al., On the high energy emission of the short GRB 090510, Astrophys. J. (2010), in press, arXiv:1009.1432.
[328] R.-Y. Liu, X.-Y. Wang, Modeling the broadband emission of Fermi/LAT GRB 090902B, Astrophys. J. 730 (2011) 1, doi:10.1088/0004-637X/730/1/1, arXiv:1009.1289.
[329] Z. Li, Prompt GeV emission from residual collisions in gamma-ray burst outflows: Evidence from Fermi observations of GRB 080916C, Astrophys. J. 709 (2010) 525–534.
[330] K. Ioka, Very high Lorentz factor fireballs and gamma-ray burst spectra, Prog. Theor. Phys. 124 (2010) 667–710.
[331] M. De Pasquale, et al., Swift and Fermi observations of the early afterglow of the short gamma-ray burst 090510, Astrophys. J. 709 (2010) L146–L151.
[332] A.M. Hopkins, J.F. Beacom, On the normalization of the cosmic star formation history, Astrophys. J. 651 (2006) 142–154.
[333] M.D. Kistler, et al., An unexpectedly Swift rise in the gamma-ray burst rate, Astrophys. J. 673 (2008) L119–L122.
[334] V. Bromm, A. Loeb, High-redshift gamma-ray bursts from Population III progenitors, Astrophys. J. 642 (2006) 382–388.
[335] N.R. Butler, J.S. Bloom, D. Poznanski, The cosmic rate, luminosity function, and intrinsic correlations of long gamma-ray bursts, Astrophys. J. 711 (2010) 495–516.
[336] S.-F. Qin, et al., Simulations on high-z long gamma-ray burst rate, Month. Not. Roy. Astron. Soc. 406 (2010) 558–565.
[337] F. Virgili, et al., in preparation.
[338] M.A. Campisi, et al., Properties of long gamma-ray burst host galaxies in cosmological simulations, Month. Not. Roy. Astron. Soc. 400 (2009) 1613–1624.
[339] G.P. Holder, et al., The reionization history at high redshifts. II. Estimating the optical depth to Thomson scattering from cosmic microwave background polarization, Astrophys. J. 595 (2003) 13–18.
[340] X. Fan, C.L. Carilli, B. Keating, Observational constraints on cosmic reionization, Annu. Rev. Astron. Astrophys. 44 (2006) 415–462.
[341] T. Totani, et al., Implications for cosmic reionization from the optical afterglow spectrum of the gamma-ray burst 050904 at $z = 6.3$, Publ. Astron. Soc. Jpn. 58 (2006) 485–498.
[342] K. Nagamine, B. Zhang, L. Hernquist, Incidence rate of GRB-host DLAs at high redshift, Astrophys. J. 686 (2008) L57–L60.
[343] A. Pontzen, et al., The nature of HI absorbers in gamma-ray burst afterglows: clues from hydrodynamic simulations, Month. Not. Roy. Astron. Soc. 402 (2010) 1523–1535.
[344] T. Abel, G.L. Bryan, M.L. Norman, The formation of the first star in the universe, Science 295 (2002) 93–98.
[345] S.S. Komissarov, M.V. Barkov, Supercollapsars and their X-ray bursts, Month. Not. Roy. Astron. Soc. 402 (2010) L25–L29.
[346] P. Mészáros, M.J. Rees, Population III gamma-ray bursts, Astrophys. J. 715 (2010) 967–971.
[347] M.J. Turk, T. Abel, B. O'Shea, The formation of Population III binaries from cosmological initial conditions, Science 325 (2009) 601–603.
[348] A. Janiuk, D. Proga, Low angular momentum accretion in the collapsar: How long can a long GRB be?, Astrophys. J. 675 (2008) 519–527.
[349] A. Janiuk, R. Moderski, D. Proga, On the duration of long GRBs: Effects of black hole spin, Astrophys. J. 687 (2008) 433–442.
[350] P. Petitjean, S.D. Vergani, Gamma-ray bursts as probes of the distant Universe, C. R. Physique 12 (2011) 288–297 (this issue).
[351] R. Yamazaki, Prior emission model for X-ray plateau phase of gamma-ray burst afterglows, Astrophys. J. 690 (2009) L118–L121.
[352] E.-W. Liang, et al., A comprehensive analysis of Swift/X-ray telescope data. IV. Single power-law decaying light curves versus canonical light curves and implications for a unified origin of X-rays, Astrophys. J. 707 (2009) 328–342.